JOC The Journal of Organic Chemistry

Article

pubs.acs.org/joc

Steric Effects in the Tuning of the Diastereoselectivity of the Intramolecular Free-Radical Cyclization to an Olefin As Exemplified through the Synthesis of a Carba-Pentofuranose Scaffold

Mansoureh Karimiahmadabadi, Sayeh Erfan, Andras Földesi, and Jyoti Chattopadhyaya*

Program of Chemical Biology, Department of Cell and Molecular Biology, Biomedical Centre, Uppsala University, SE-75123 Uppsala, Sweden

Supporting Information

ABSTRACT: Two free-radical cyclization reactions with the radical at the chiral C4 of the pentose sugar and the intramolecularly C1-tethered olefin (on radical precursors **8** and **17**) gave a new diastereospecific C4−C8 bond in dimethylbicyclo[2.2.1]heptane **9**, whereas the new C4−C7 bond in 7-methyl-2-oxabicyclo[2.2.1]heptanes **18a**/**18b** gave *trans* and *cis* diastereomers, in which the chirality of the C4 center is fully retained as that of the starting material. It has been shown how the chemical nature of the fused carba-pentofuranose scaffolds, dimethylbicyclo[2.2.1]heptane **9** vis-a-vis 7-methyl-2-oxabicyclo[2.2.1]heptanes **18a**/**18b** (C7-Me in the former versus 2-*O*- in the latter), dictates the stereochemical outcome both at the Grignard reaction step as well as in the free-radical ring-closure reaction. The formation of pure 1,8-*trans*-bicyclo[2.2.1]heptane **9** from **8** suggests that the boat-like transition state is favored due to the absence of steric clash of the bulky 1(*S*)-*O*-*p*-methoxybenzyl (PMB) and 7(*R*)-Me substituents (both in the α-face) with that of the 8(*R*)-$CH_2^{\bullet}$ radical in the β-face. The conversion of **17** → **18a**-7(*S*) and **18b**-7(*R*) in 6:4 ratio shows that the participation of both the chair- and the boat-like transition states is likely.

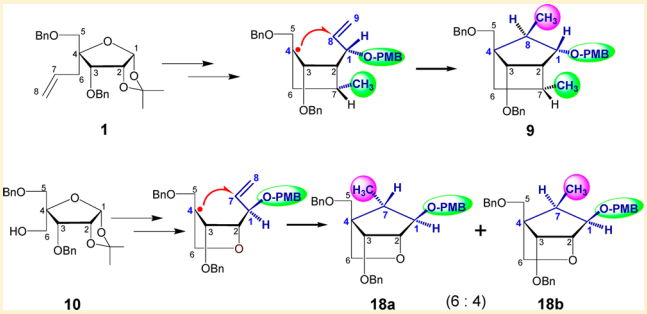

INTRODUCTION

Recently, we have shown that substitution of 2′-*O*- in LNA (locked nucleic acid: 2′-*O*,4′-*C*-methylenebicyclonucleoside)[1a,b] by the 2′-CH(Me)- group, giving carbocyclic nucleosides (carba-LNA),[1c−i] enhances the nucleolytic stability of the carba-LNA-modified oligo-DNA or RNA by ∼145 times.[1f] These carba-LNA-modified small interfering RNAs (siRNA) have been found to be useful as potential therapeutic agents against HIV-1,[2,3] whereas the carba-LNA-modified antisense oligonucleotides are found to be active against allele-specific Huntington disease,[4] owing to improved target RNA affinity, single-mismatch discrimination, and nuclease stability.[1c−e]

On the other hand, the cyclopentane nucleoside derivative in which the furanose O4′-oxygen is replaced by methylene stabilizes the glycosidic bond and enhances the biological stability,[5,6] which in turn culminates into enhanced selectivity to different viral enzymes.[5e,f] Thus, the locked North-type (N) methanocarba-adenosine analogues[6] showed favorable pharmacodynamic properties in binding assays to A1, A_{2A}, and A3 receptors compared to the S-locked analogue.[6] The syntheses of several carbocyclic nucleosides have been reported so far.[7a,b] They used different (Grubb's[7a] and Schrock's catalyst[8]) metathesis approaches for closing the carba-ring to give functionalized cyclopentanol. Synthesis of annulated furanoses[9] was reported through the radical cyclization to the intramolecularly tethered olefin (Table 1, compounds **II**, **IV**, **VI**, and **VIII**).[10] The radical was always generated at a nonchiral carbon center to avoid the generation of an intractable mixture of diastereomers owing to epimerization during the radical addition reaction. However, when the radical was generated at the nonchiral centers of the furanose ring (**I** → **II**), or at its side chain, a diastereomeric mixture of *cis* and *trans* isomers (**III** → **IV** and **V** → **VI**)[11] was obtained. When the radical was generated at a nonchiral carbon and had a constrained olefin in the proximity, which was part of a ring, it gave a diastereomerically pure isomer as shown by conversion of **VII** → **VIII** (74%) and **IX** → **X** (76%),[11] owing to steric reasons.

A radical center generated at an achiral carbon added easily to a C═N of an oximino ether (**VII**) to give 1-benzyloxyaminocyclopentane (**VIII**) as a diastereomerically pure main product in 74% yield. All of these reactions, **VII** → **VIII** and **IX** → **X**, took place by 5-*exo* ring closure and gave one major isomer because of the steric effect imposed by the acetonide group on the α-face of the pentose sugar ring. However, the alkyl substitution at the radical center and ring strain have been shown to promote the radical 6-*endo* cyclization (**XI** → **XII**), thereby allowing syntheses of carba-pyranoses from a carbohydrate precursor. Similarly, a vinyl radical led to more 6-*endo* cyclization (**XIII** → **XIV** + **XV**,

Received: May 9, 2012
Published: August 2, 2012

Table 1. Formation of Annulated Furanoses and Carba-Pyranoses through the Free-Radical Cyclization Reaction in Which the Radical Generated Is Invariably on the Nonchiral Carbon

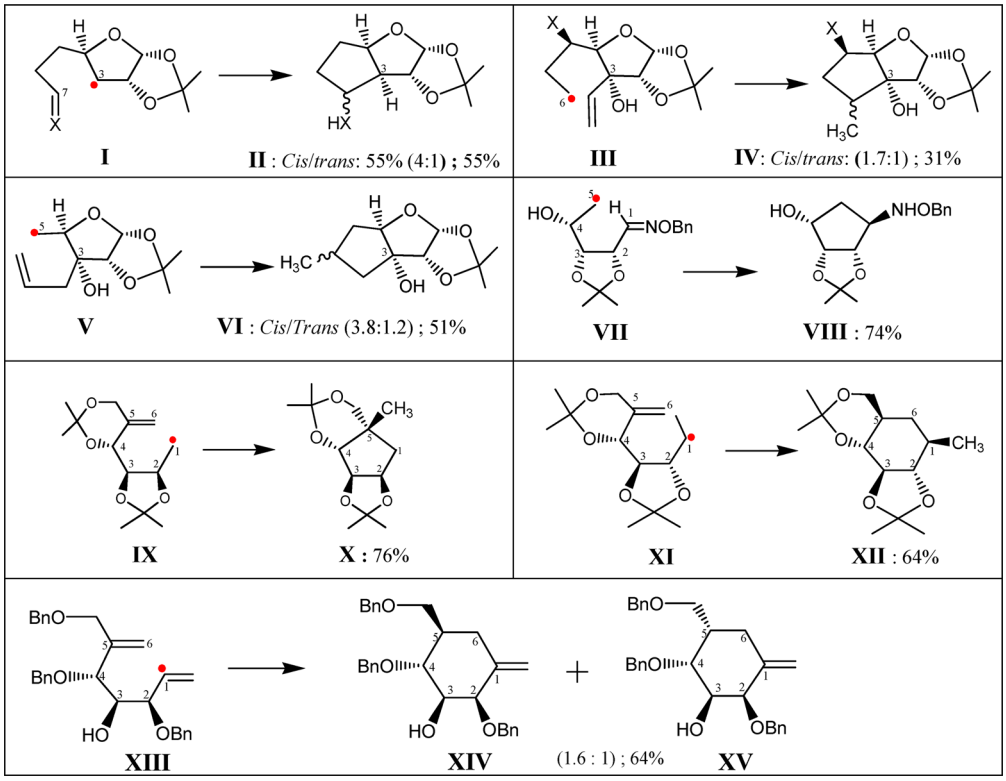

Scheme 1. Retrosynthetic Routes

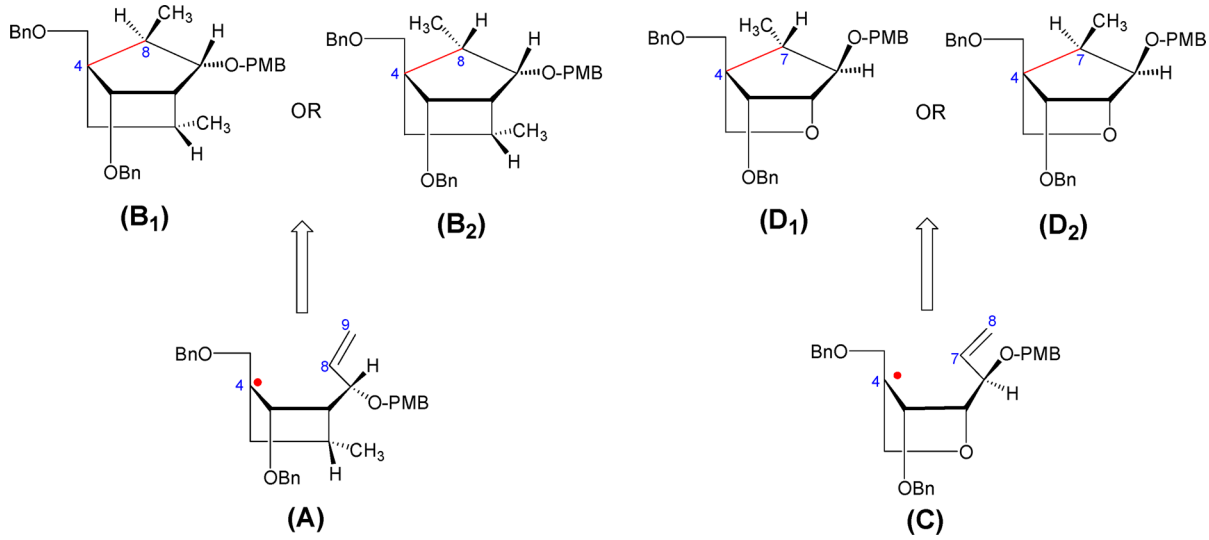

1.6:1), whereas an alkyl radical in compound **IX** gave only the *exo* cyclization product **X**.

Beckwith,[12] Houk,[13] and Rajan Babu[14] have reported that hex-5-enyl radical cyclization generally proceeds through a chair-like or boat-like transition state with very low energy barrier.[1c] Whether a chair- or boat-like transition state would actually be involved in the product formation depends upon many other stereochemical effectors around these two transition states,[1c,14] which may compensate for the formation of the normally unfavorable boat-like transition state or actually provide extra stabilization of the chair-like transition state.

We herein report a radical ring-closure reaction in which the radical is generated at the chiral center with an intramolecularly tethered olefin to give appropriately functionalized carba-D-furanose.

RESULTS AND DISCUSSION

Clearly, the free-radical generated at the chiral C4 center of a D-furanose ring by a 5-*exo* ring-closure reaction to an intramolecularly tethered olefin is likely to give a D and L diastereomeric mixture, unless the C4 center is actually a part of a ring. Hence in order to retain the D configuration of the newly formed carba-ring, we argued that construction of a C2 to

dx.doi.org/10.1021/jo300936g | J. Org. Chem. 2012, 77, 6855−6872

Scheme 2. Synthesis of the (1*S*,2*R*,3*S*,4*R*,7*R*,8*R*)-3-(Benzyloxy)-4-[benzyloxymethyl]-1-[(4-methyloxyphenyl)methoxy]-8,7-dimethylbicyclo[2.2.1]heptane (9)

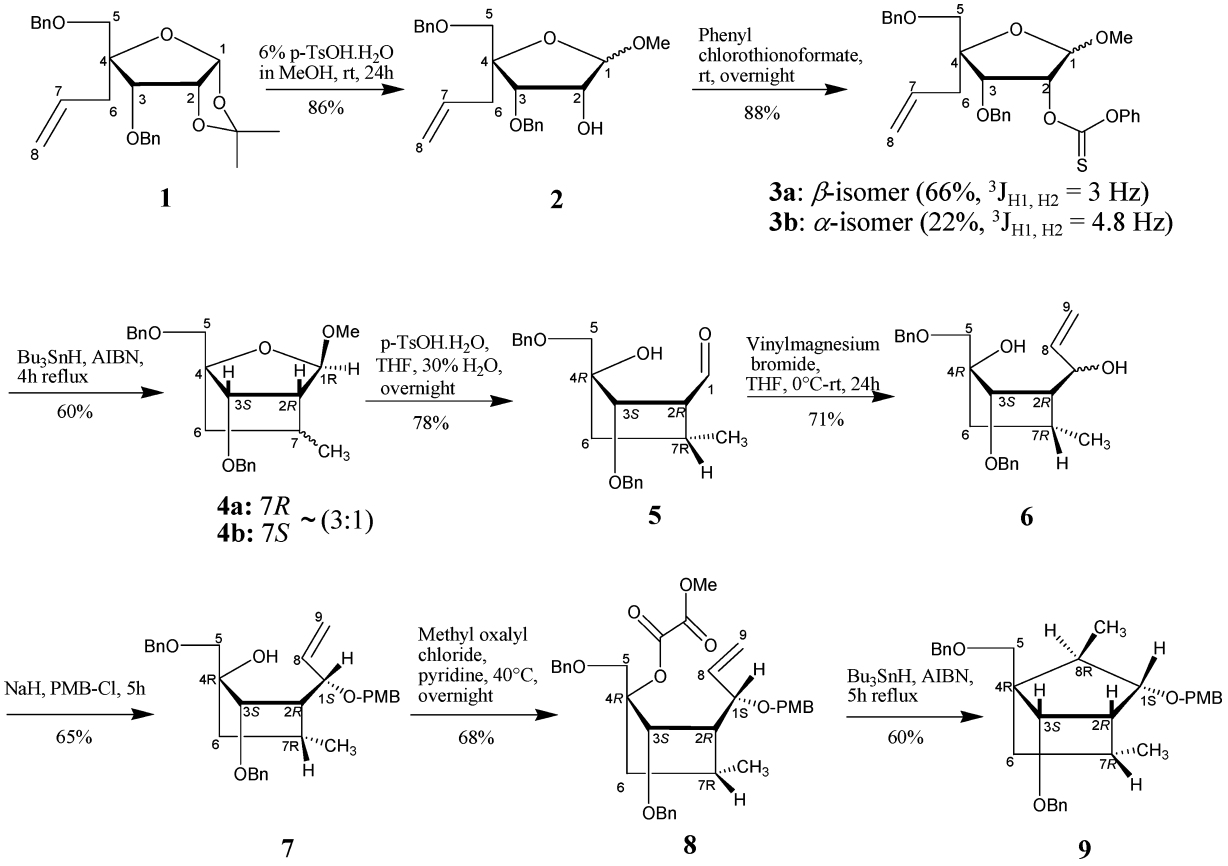

C4 bridge as in dimethylbicyclo[2.2.1]heptanes $\mathbf{B_1}$ and $\mathbf{B_2}$ or a furano bridge (oxabicyclo bridge [2.2.1]) as in $\mathbf{D_1}$ and $\mathbf{D_2}$ (Scheme 1) will be necessary in order to stop the formation of diastereomers at the chiral C4 center. It was also clear that the intramolecular 5-*exo* ring closure by the C4 radical center to the C8 of the tethered olefin (**A**→ $\mathbf{B_1}$ or $\mathbf{B_2}$) or to the C7 center of the olefin (**C** → $\mathbf{D_1}$ or $\mathbf{D_2}$) will create two new chiral centers across the C4−C8 or C4−C7 bond (as in $\mathbf{B_1}$ or $\mathbf{B_2}$ and $\mathbf{D_1}$ or $\mathbf{D_2}$, respectively). As we wish to understand the steric factors that control the stereochemistry of the radical ring closure, we tried to influence the participation of either chair- or boat-like forms to give *cis* and/or *trans* cyclic products, respectively, across the C4 and C8 centers.

This prompted us to attempt two free-radical cyclization reactions, first, on 3-(1-hydroxyallyl)-cyclopentanol derivative (**A**) to give 7,8-dimethylbicyclo[2.2.1]heptanes ($\mathbf{B_1}$ or $\mathbf{B_2}$) and, second, on **C** to give 7-methyl-2-oxabicyclo[2.2.1]heptanes ($\mathbf{D_1}$ or $\mathbf{D_2}$).

Synthesis of the (1*S*,2*R*,3*S*,4*R*,7*R*,8*R*)-3-(Benzyloxy)-4-[benzyloxymethyl]-1-[(4-methyloxyphenyl)methoxy]-8,7-dimethylbicyclo[2.2.1]heptane (9). The synthesis of carbocyclic pentose **9** starts from the known 4-*C*-allyl-3,5-di-*O*-benzyl-1,2-*O*-isopropylidene-α-D-ribofuranose **1**[1d] (Scheme 2). Compound **1** was treated with *p*-toluenesulfonic acid·H_2O in MeOH to obtain the methyl glycoside **2** in a one-pot reaction[15] as an inseparable mixture of α- and β-anomers in 86% yield. The ^{1}H NMR assignment approximately shows a 4:1 ratio of the two anomers (Figure S1, Supporting Information part I). After 2-esterification of the α and β mixture **2** with phenyl chlorothionoformate in dry pyridine at room temperature, the key intermediates for the radical cyclization, 2-*O*-phenoxythiocarbonyl **3a** (β-isomer, 66%, $[\alpha]_D^{25}$ = −52) (Figures S6−S10, Supporting Information part I) and **3b** (α-isomer, 22%, $[\alpha]_D^{25}$ = −14), (Figures S11−S15, Supporting Information part I) were separated as pure isomers. Their structures were confirmed by both coupling constant analysis and nuclear Overhauser effect (NOE) experiments. For compound **3a** (β-isomer), the $^3J_{H1,H2}$ = 3 ± 0.2 Hz (Figure S6, Supporting Information part I) suggests a *transoid* orientation for H1 and H2 (Figure 1, panel A_1 for Newman projection), thereby suggesting a 1(*R*) configuration for **3a**.

In a similar way, the $^3J_{H1,H2}$ = 4.8 ± 0.2 Hz (Figure S11, Supporting Information part I) was assigned for the α-isomer (Figure 1, panel B_1 for Newman projection) for *cis* orientation (eclipsed) between H1 and H2 [1(*S*) configuration] for **3b**. The stereochemistry at C1 was further confirmed by NOE: for the β-isomer, the irradiation of H2 (Figure 1, panel A_1) shows 1.6% NOE enhancement for H1 ($d_{H1,H2(calc)} \approx 2.9$ Å) which shows (*R*) configuration at C1. In contrast, the irradiation of H2 (Figure 1, panel B_1) in the α-isomer gave a strong NOE enhancement for H1, 3.4% ($d_{H1,H2(calc)} \approx 2.3$ Å), which shows that H1 and H2 are *cis* and C1 is with (*S*) configuration.

The products **3a** and **3b** were subjected to the radical ring closure in degassed anhydrous toluene at reflux temperature in the presence of Bu_3SnH, while azobisisobutyronitrile (AIBN) was added dropwise as radical initiator using our procedure.[1d] Quite expectedly, the β-isomer **3a** successfully afforded a diastereomeric mixture of two isomers **4a** (Figures S16−S21, Supporting Information part I) and **4b** (Figures S22−S26, Supporting Information part I) (60% yield) through the 5-*exo*

dx.doi.org/10.1021/jo300936g | J. Org. Chem. 2012, 77, 6855−6872

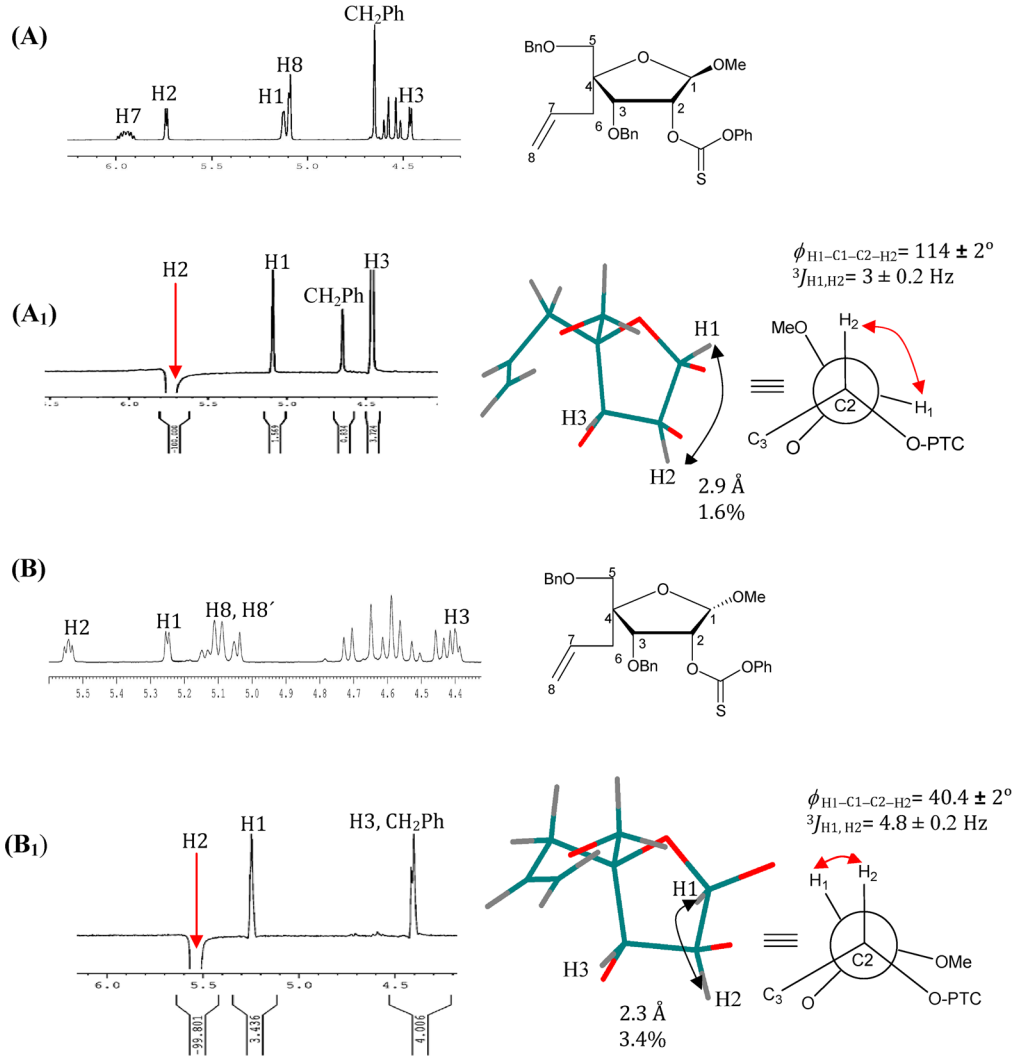

Figure 1. ^{1}H NMR of the (A) β-isomer **3a** and (B) α-isomer **3b** and (A_1,B_1) NOEs observed upon irradiation of their respective H2, thereby confirming the configuration at C1 to be β in **3a** and α in **3b**, respectively.

cyclization. The ^{1}H NMR assignment approximately shows a 3:1 ratio of the two isomers **4a** and **4b**. The major isomer **4a**, $[\alpha]_D^{25}$ = −21, could be isolated in the pure form, but the minor isomer **4b** contained a 30% impurity of **4a**.

The radical cyclization can proceed through a chair- or a boat-like transition state (Figure 2) where the former is favored. On the other hand, a bulky substituent at the centers close to the radical center might influence the stereochemical outcome in order to increase the product with less steric interaction (the boat-like TS), which is the result in this case.

The boat-like TS1 is favorable due to the absence of the clash between 7(*R*)-Me and the axial 3(*S*)-OBn which leads to the 2,7-*cis* product (Figure 2, panel A). In contrast, the clash between the 7(*S*)-Me and the axial 3(*S*)-OBn makes the chair-like TS3 (gives the 2,7-*trans* product) less favored (Figure 2, panel B). The formation of the new C2−C7 bond has been corroborated by the presence of the correlation between H2 and H7 in the COSY experiment (Figure S21, panel A, in Supporting Information part I). The HMBC correlation spectra (Figure S21, panel B, in Supporting Information part I) provided further evidence through the cross-peaks between H1 and C7 due to the long-range ^{1}H−^{13}C coupling over the C2−C7 bond, thereby confirming the presence of the new C2−C7 bond in **4a**. The stereochemistry of the new chiral center, C7, has been assigned by NOE enhancement (Figure S27, panel A_1, in Supporting Information part I) and coupling constant analysis for major isomer **4a**: irradiation of H1 led to 3.7% NOE enhancement for 7-Me ($d_{H1,7\text{-Me(calc)}} \approx 2.2$ Å), but the weak NOE enhancement for H7 (0.3%, $d_{H1,H7(calc)} \approx 3.8$ Å) suggested that the H1 and 7-Me were oriented on the same face of the [2.2.1]-fused carba-ring, which means that H2 and H7 are *cis* to each other.

This was further evidenced by the coupling constant analysis of **4a** which shows $^3J_{H2,H7}$ = 3 ± 0.2 Hz (Figure S27, panel A_1, in Supporting Information part I for Newman projection), thereby confirming 7(*R*) and 2(*R*) configurations for the carbo-pentose **4a**. The stereochemistry of the new chiral center at C7 for the minor isomer **4b** has also been determined by NOE (Figure S27, panels B_1 and B_2, in Supporting Information part I): irradiation of 7-Me showed a weak NOE enhancement for H1 (0.4%, $d_{H1,7\text{-Me(calc)}} \approx 4.2$ Å), but irradiation of H7 led to a strong NOE enhancement for H1 (3.7%, $d_{H7,H1(calc)} \approx 2.2$ Å), which suggests that H7 and H1 are oriented on the same face of the carba-ring, thereby confirming 7(*S*) and 2(*R*) configurations for the carba-pentose **4b**.

An effort to produce the 5-*exo*-cyclized compound from the α-isomer **3b** was unsuccessful; this is likely due to the steric

dx.doi.org/10.1021/jo300936g | J. Org. Chem. 2012, 77, 6855−6872

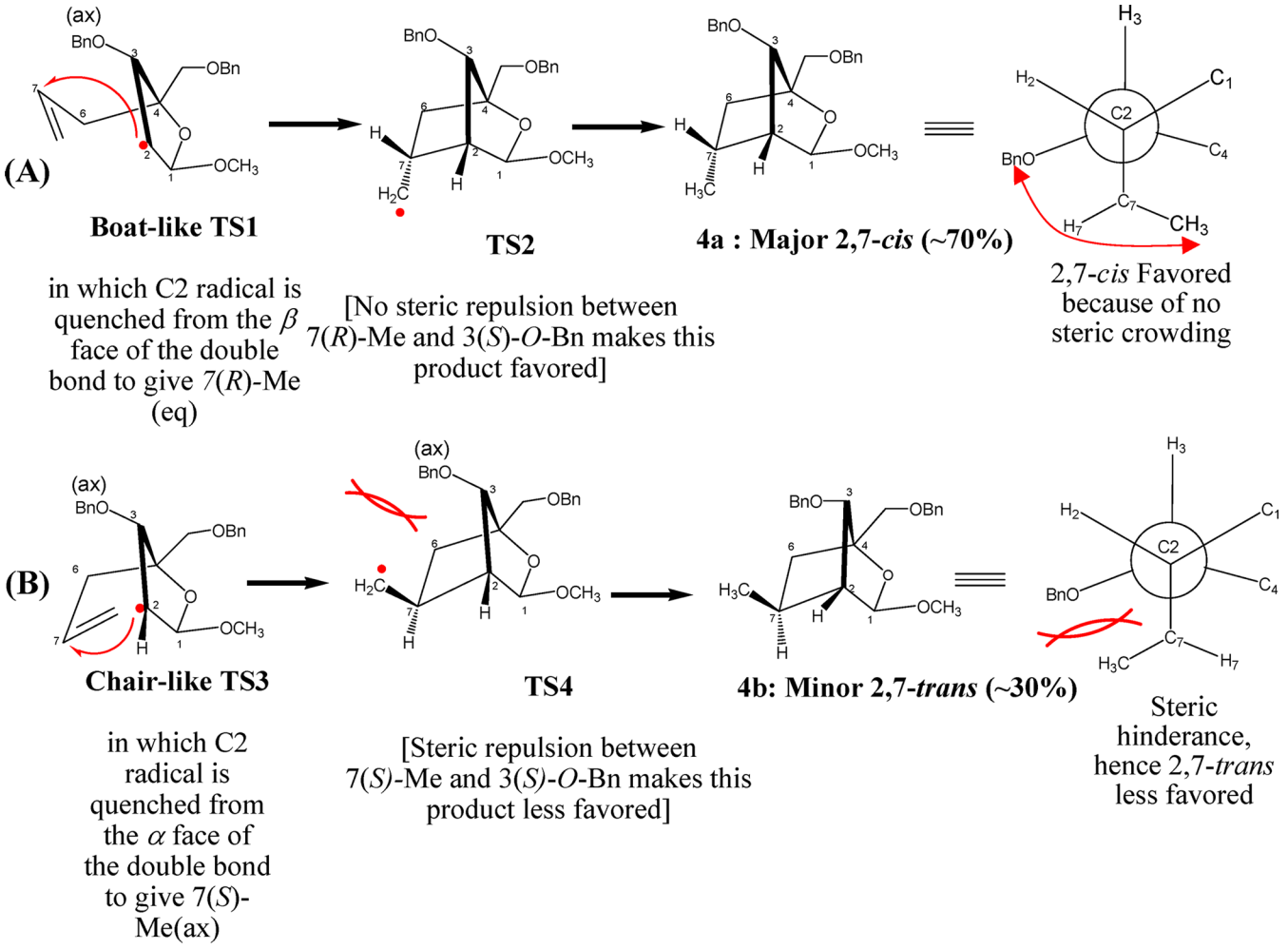

Figure 2. Mechanism of the stereoselectivity of the 5-*exo* radical ring-closure reaction to a tethered olefin, in which the 2,7-*cis* addition, **4a**, is favored over the 2,7-*trans* addition, **4b**, owing to the presence or absence of steric crowding.[1c]

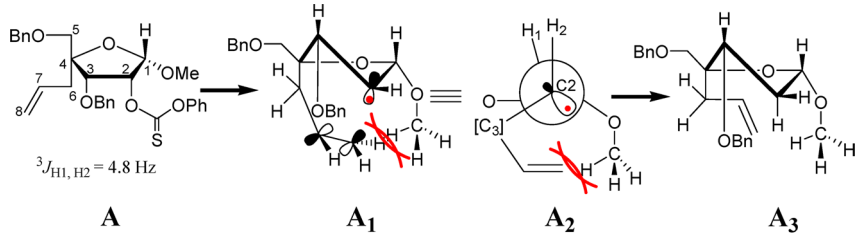

Figure 3. Due to the steric hindrance by the 1-methoxy group, the incipient radical at C2 in the α-isomer (in $\mathbf{A_1}$/$\mathbf{A_2}$) cannot attack the double bond.

hindrance of 1-methoxy group (Figure 3) on the α-face of the pentose ring through which the radical cyclization takes place in the β-isomer **3a** → **4**. Hence, the radical generated at C2 in **3b** was found to be quenched by a hydrogen atom to give the 2-deoxygenated compound $\mathbf{A_3}$ before it could be captured by the double bond (Figure 3).

Compound **4** was hydrolyzed by a 30% aqueous mixture of *p*-toluenesulfonic acid·H_2O in THF at room temperature to give the aldehyde **5** in 78% yield (Figures S28 and S29, Supporting Information part I). The aldehyde **5** was then subjected to a Grignard reaction using vinylmagnesium bromide (4 equiv) at room temperature in dry THF overnight to produce the alkene-diol **6** (71%), (Figures S30−S34, Supporting Information part I) as an inseparable mixture of two isomers with a single spot on TLC. The ^{1}H NMR assignment approximately shows 5:1 ratio of the two isomers. Compound **6** was selectively protected at C1-OH with a bulky *p*-methoxybenzyl (PMB) group using NaH and PMB-Cl (1.2 equiv) in dry DMF at 0 °C to obtain the desired 1-*O*-PMB product **7** (Figures S35−S39, Supporting Information part I) (65%, $[\alpha]_D^{25} = -27$). At this stage, we succeeded to isolate only the major isomer **7**. The stereochemistry of this compound has been assigned by coupling constant analysis and NOE experiments: homonuclear decoupling of H8 shows the $^3J_{H1,H2}$ = 3.5 ± 0.2 Hz, suggesting a *cis* relationship between H1 and H2 (Figure S54 in Supporting Information part I) with C1(*S*) configuration. The $^3J_{H1,H8}$ = 7.5 ± 0.2 Hz (Figure S55 in Supporting Information part I) was assigned for the *trans* orientation between H1 and H8. The $^3J_{H2,H7}$ = 8.5 ± 0.2 Hz shows *cis* relationship between H2 and H7 (Figure S57 in Supporting Information part I), which suggests (*R*) config-

dx.doi.org/10.1021/jo300936g | J. Org. Chem. 2012, 77, 6855−6872

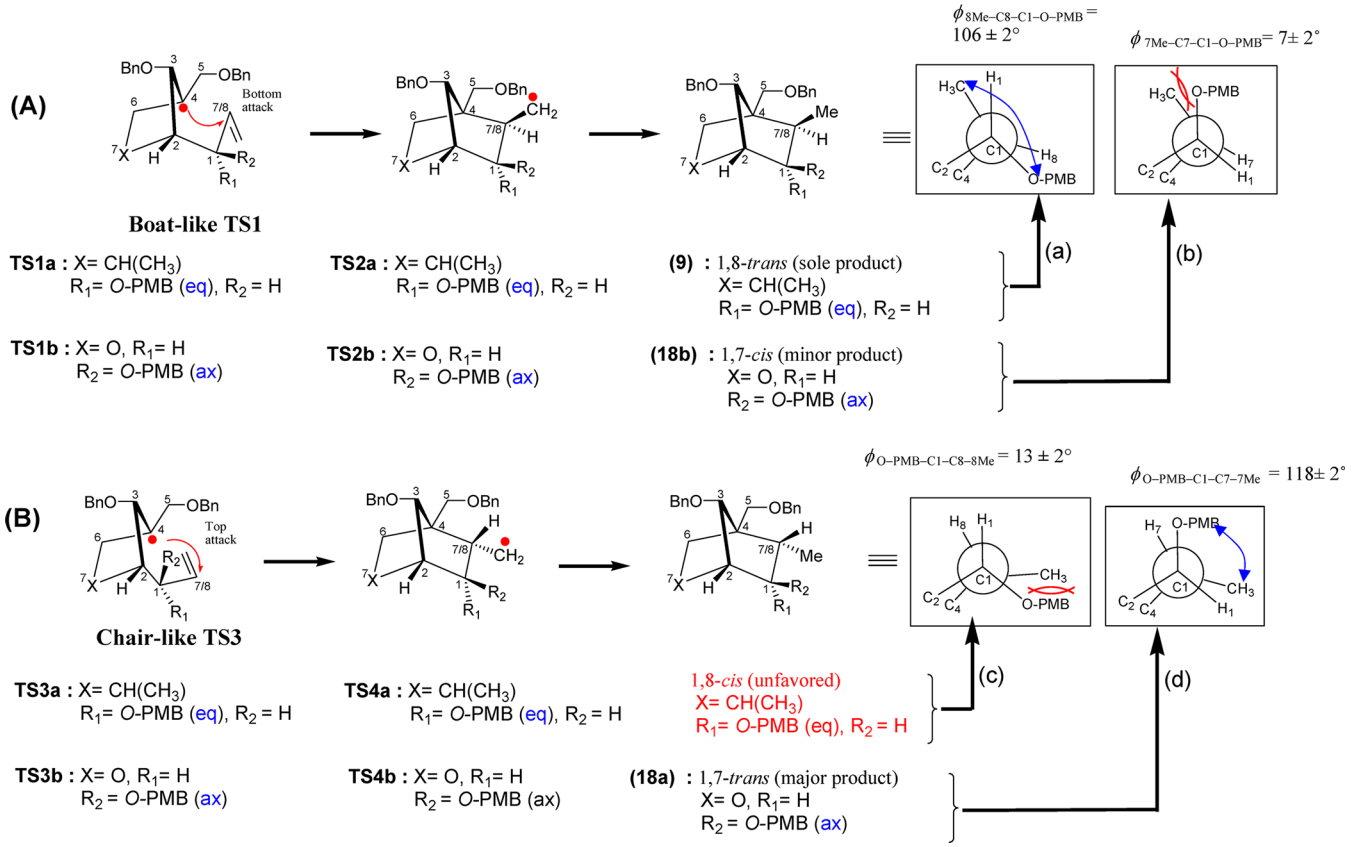

Figure 4. (A) TS1a (boat-like conformation) in which there is no steric repulsion between the *trans*-oriented 1-(*S*)-*O*-PMB (eq) and 8-Me (ax), thereby giving the sole 1,8-*trans* product **9**. TS1b in panel A (boat-like conformation) shows that the steric repulsion between the *cis*-oriented 1-(*R*)-*O*-PMB (ax) and 7-Me (ax) giving the thermodynamically less favorable 1,7-*cis* product **18b**. (B) Chair-like TS3a shows that because of the steric repulsion between the *cis*-oriented 1-(*S*)-*O*-PMB (eq) and 7-Me (ax), the 1,8-*cis* product is disfavored. On the other hand, TS3b shows that a chair-like conformation in TS3b involves no steric clash between the *trans*-oriented 1-(*R*)-*O*-PMB (ax) and 7-Me (eq), thereby giving the favorable 1,7-*trans* product **18a**.

uration at the C7 center. These results have been further evidenced by NOE enhancements: irradiation of H8 (Figure S51 in Supporting Information part I) led to NOE enhancement for H3 [1.4%, $d_{H8,H3(calc)} \approx 2.7$ Å] and H2 [1.4%, $d_{H8,H2(calc)} \approx 3.4$ Å], which confirms that H8, H2, and H3 were oriented on the same face of the pentose sugar (β-face), which means that Grignard addition to 1-CH═O takes place from the β-face, that is, from the top of the 1-CH═O, and C1 possess an (*S*) configuration. In contradistinction, if the Grignard addition to 1-CH═O were to take place from its α-face (*i.e.*, from the bottom of the 1-CH═O), we should not have observed any NOE between H8 of the olefin and H3 of the sugar since $d_{H8,H3(calc)}$ is ≈4.6 Å (modeled by HyperChem, MM/Amber, and semiempirical/AM1; see Experimental Section). Further confirmation comes from irradiation of H1 (Figure S52 in Supporting Information part I), which shows 3.6% NOE enhancement for H2 ($d_{H1,H2(calc)} \approx 2.5$ Å), thereby suggesting that H1 and H2 are on the β-face with *cis* orientation.

Compound **7** was subjected to esterification at 4-OH with methyl(chlorocarbonyl)formate in pyridine at 40 °C overnight to give the key precursor **8** (68%, $[\alpha]_D^{25} = -33$) for the free-radical cyclization. The configuration of the intermediate **8** was also confirmed by coupling constant and NOE experiments: the $^3J_{H1,H8} = 7.5 \pm 0.2$ Hz was found for compound **8** (Figure S62 in Supporting Information part I), which suggests *trans* orientation between H1 and H8. The $^3J_{H2,H7} = 8 \pm 0.2$ Hz indicates *cis* relationship between H2 and H7 (Figure S63 in Supporting Information part I), which gives (*R*) configuration at the C7 center. These assignments have been further evidenced by the NOEs: irradiation of H1 (Figure S61 in Supporting Information part I) shows 2.4% NOE enhancement for H2 ($d_{H1,H2(calc)} \approx 2.4$ Å), suggesting that H1 and H2 are on the same face [*cis* orientation, 1(*S*) configuration]. Irradiation of H8 (Figure S59 in Supporting Information part I) led to NOE enhancement for H3 [1.6%, $d_{H8,H3(calc)} \approx 2.4$ Å] and H2 [1.7%, $d_{H8,H2(calc)} \approx 3.4$ Å], which confirms that H8, H2, and H3 are oriented on the same face of the alkene group.

The key intermediate **8** was subjected to radical cyclization in anhydrous toluene under reflux by dropwise addition of Bu_3SnH (4 equiv), utilizing AIBN as the initiator during 4 h to avoid the C4-deoxygenation product formation. The hexenyl radical cyclization at C8 proceeded in the 5-*exo* cyclization mode to give only one [2.2.1]-fused C4−C8 *trans*-fused product **9**, with 8(*R*) configuration as the main product (60%, $[\alpha]_D^{25} = 32$), along with the C4-deoxygenated product. The stereospecificity of the radical reaction is due to the absence of steric hindrance of the 1-*O*-PMB group and the 7(*R*)-Me group which drives the 8(*R*)-$CH_2^\bullet$ radical to the β-face (TS1a and TS2a in Figure 4). In addition, 1D NOE experiments (Figure 5) confirm the configuration which showed to be (*S*) at C1 and (*R*) at C4. Hence, these two centers preserved their configuration after radical reaction. However, the C8 was not a chiral center in the starting material, but after the radical reaction, the chiral center was generated to be of (*R*) configuration.

Mechanism of the 5-*exo* Free-Radical Cyclization To Give (1*S*,2*R*,3*S*,4*R*,7*R*,8*R*)-3-(Benzyloxy)-4-[benzyloxy-

dx.doi.org/10.1021/jo300936g | *J. Org. Chem.* 2012, 77, 6855−6872

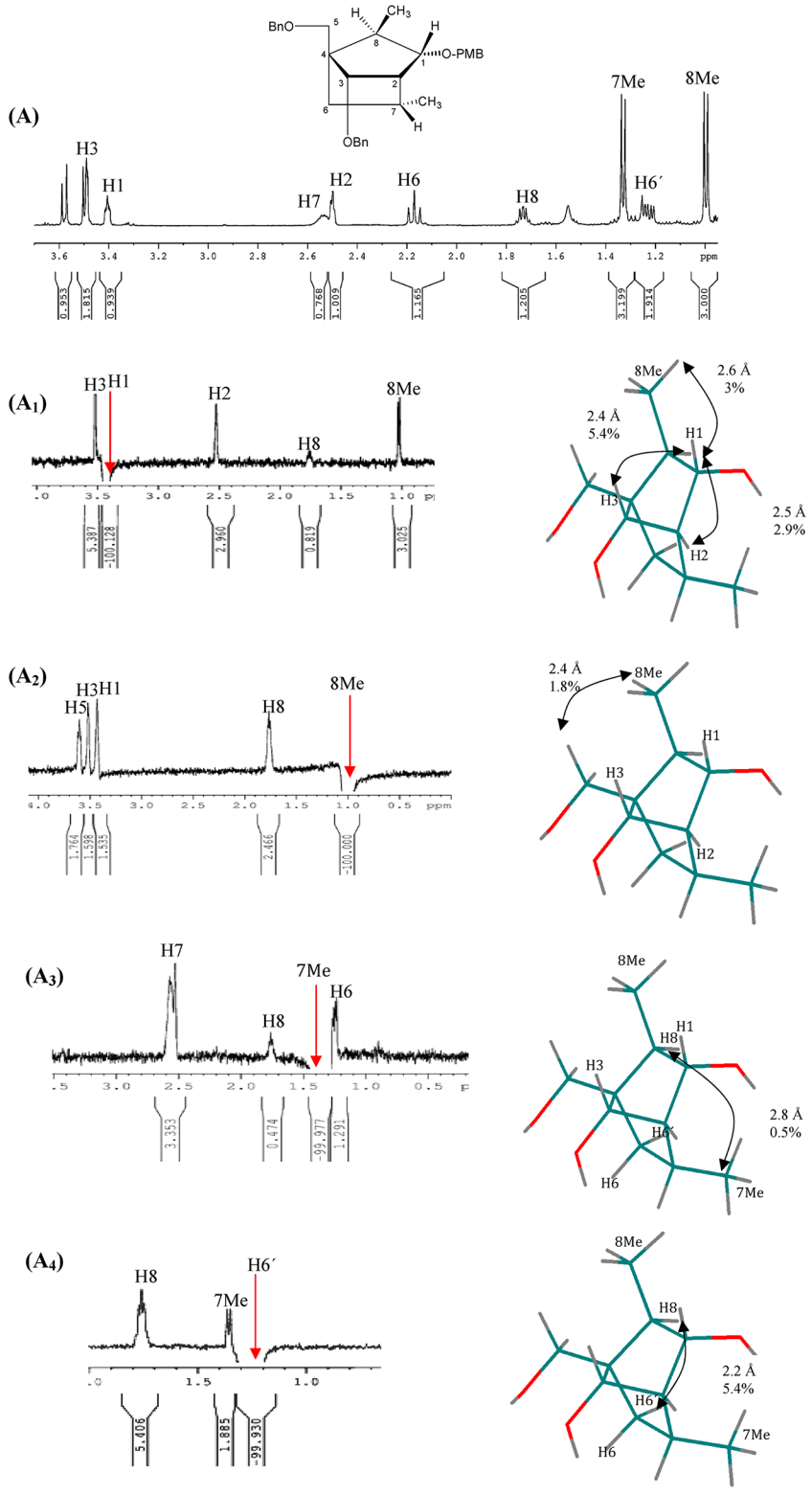

Figure 5. (A) ^{1}H NMR spectrum (600 MHz) of compound **9**. (A_1,A_2) NOE enhancements of compound **9**; irradiation of H1 showed 5.4% NOE enhancements for H3, and irradiation of 8(*R*)-Me shows 1.8% NOE enhancement with H5, which indicated that 8(*R*)-Me and H5 are on the *β*-face of the carba-sugar, thereby proving the configuration of C8 to be (*R*). (A_3,A_4) Irradiation of 7(*R*)-Me shows 0.5% NOE enhancement for H8, but none for 8(*R*)-Me, and irradiation of H6′ shows 5.4% NOE enhancement with H8, which shows that the 8(*R*)-Me is on the *β*-face and the 7(*R*)-Me is on the *α*-face of the carba-sugar.

methyl]-1-[4-(methyloxyphenyl)methoxy]-8,7-dimethylbicyclo[2.2.1]heptane (9) from Methylcyclopentenyl Methyl Oxalate Derivative 8. The 5-*exo* intramoleculer cyclization of the radical generated at C4 to the C1-tethered olefin, as in **8** exclusively proceeded through the 4,8 ring closure to give **9** (Scheme 2 and Figure 4). This could be explained by Beckwith's hypothesis,[12] which enumerates the role of steric and thermodynamic factors dictating the formation of the more

dx.doi.org/10.1021/jo300936g | J. Org. Chem. 2012, 77, 6855−6872

Scheme 3. Synthesis of (1*R*,2*R*,3*R*,4*R*,7*S*)-3-(Benzyloxy)-4-[(benzyloxy)methyl]-1-[(4-methoxyphenyl)methoxy]-7-methyl-2-oxabicyclo[2.2.1]heptane (18a) and (1*R*,2*R*,3*R*,4*R*,7*R*)-3-(Benzyloxy)-4-[(benzyloxy)methyl]-1-[(4-methoxyphenyl)methoxy]-7-methyl-2-oxabicyclo[2.2.1]heptane (18b)

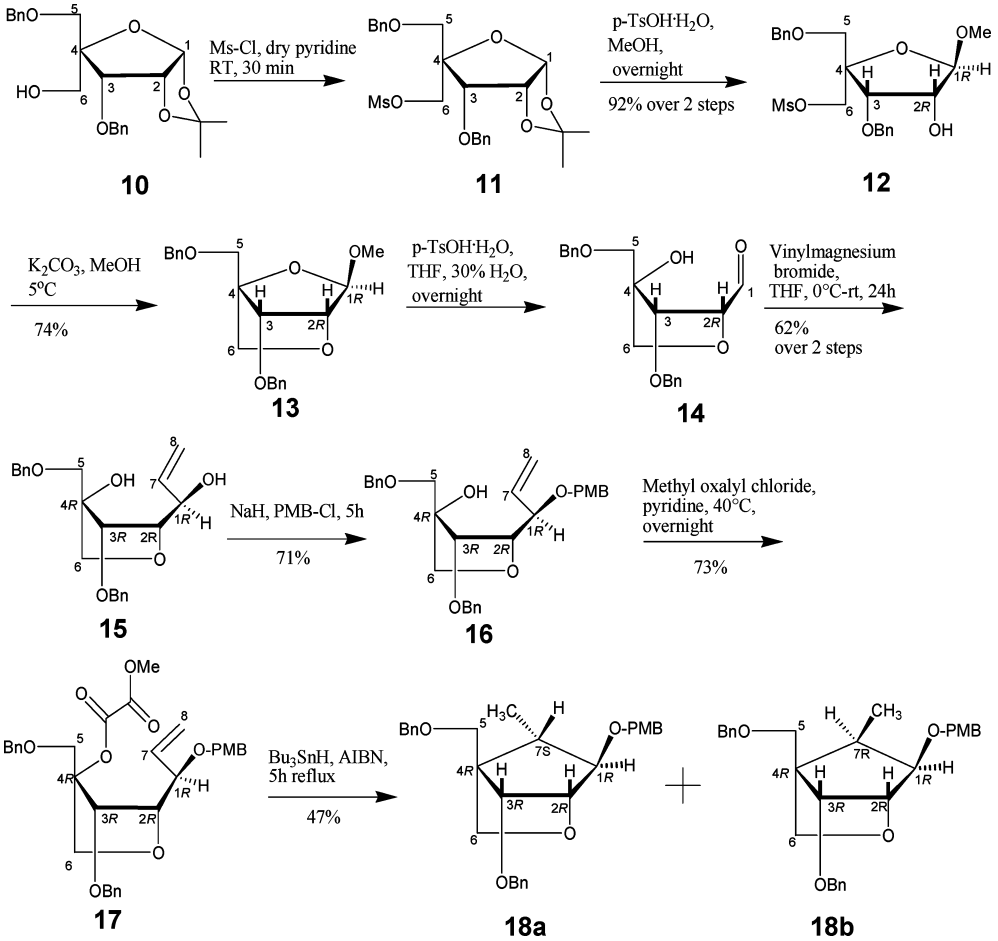

stable 5-*exo* product. Hence, no *endo* cyclization took place in our studies in the course of the ring-closure reaction. After treatment of compound **8** with AIBN and Bu_3SnH, the incipient C4 radical adopts a boat-like transition state which can attack the double bond at the α-face by involving transition states TS1a and TS2a, as schematically shown in panel A of Figure 4.

In fact, the radical cyclization can proceed through a chair- or boat-like transition state, but a bulky substituent close to the radical center may influence the stereochemical outcome in order to promote the formation of the thermodynamically stable product with relatively less steric interaction. The overlapping of SOMO of C4 with the HOMO of C8 through the boat-like transition state (Figure 4, TS1a and TS2a in panel A) drives the 8(R)-$CH_2^{\bullet}$ radical to the β-face due to absence of the steric clash of the bulky 1-*O*-PMB group and the 7(R)-Me in the α-face, thereby leading to form the 1,8-*trans* product. In contrast, in the chair-like transition state, the steric bulk of the 1-*O*-PMB group and 7(R)-Me makes the 1,8-*cis* product disfavored (Figure 4, TS3a and TS4a in panel B).

NMR Assignments To Support the Structure of (1*S*,2*R*,3*S*,4*R*,7*R*,8*R*)-3-(Benzyloxy)-4-[(benzyloxy)-methyl]-1-[(4-methyloxyphenyl)methoxy]-8,7-dimethylbicyclo[2.2.1]heptane (9). The 600 MHz ^{1}H NMR spectrum is shown in Figure 5, panel A. The doublet at δ 0.92 for 8-Me is found to be correlated with H8 (Figure S50, panel B, in Supporting Information part I) in the COSY spectrum, H8 was also found to be correlated with H1 (Figure S50, panel C, in Supporting Information part I). These observations along with the disappearance of the olefinic proton resonances (at δ 5.16 and 5.73 in the starting material) suggest that the radical generated at C4 has been quenched by the terminal double bond at C1 to give the 5-*exo* bicyclic product **9**. This was also confirmed by the observation of a long-range connectivity (HMBC) of 8-Me with C4 (Figure S50, panel D, in Supporting Information part I) and H8 with C4.

Determination of Configuration of All Chiral Centers in (1*S*,2*R*,3*S*,4*R*,7*R*,8*R*)-3-(Benzyloxy)-4-[benzyloxymethyl]-1-[(4-methyloxyphenyl)methoxy]-8,7-dimethylbicyclo-[2.2.1]heptane (9) through NOE Analysis. The configuration of the newly formed chiral center at the C8 in compound **9** has been identified by NOE experiments. Irradiation of H1 (Figure 5, panel A_1) shows a strong NOE enhancement for H3 (5.4%, $d_{H1,H3} \approx 2.4$ Å), 8-Me (3%, $d_{H1,8\text{-}Me} \approx 2.6$ Å), and H2 (2.9%, $d_{H1,H2} \approx 2.5$ Å), which confirmed that 8-Me is on the same face of the newly formed carbocycle as the original H3 and H2, which ascertained that the C8 center has (R) configuration. On the other hand, the observation of the weak NOE enhancement for H8 (0.8%, $d_{H1,H8} \approx 3$ Å) upon H1 irradiation determined that H1 and H8 are *trans*-oriented. In addition, irradiation of 8-Me (Figure 5, panel A_2) led to 1.8% NOE enhancement for H5 ($d_{8\text{-}Me,H5} \approx 2.4$ Å), which indicated that 8-Me and H5 are located on the same face. Thus, this observation confirmed the (R)

dx.doi.org/10.1021/jo300936g | *J. Org. Chem.* 2012, 77, 6855−6872

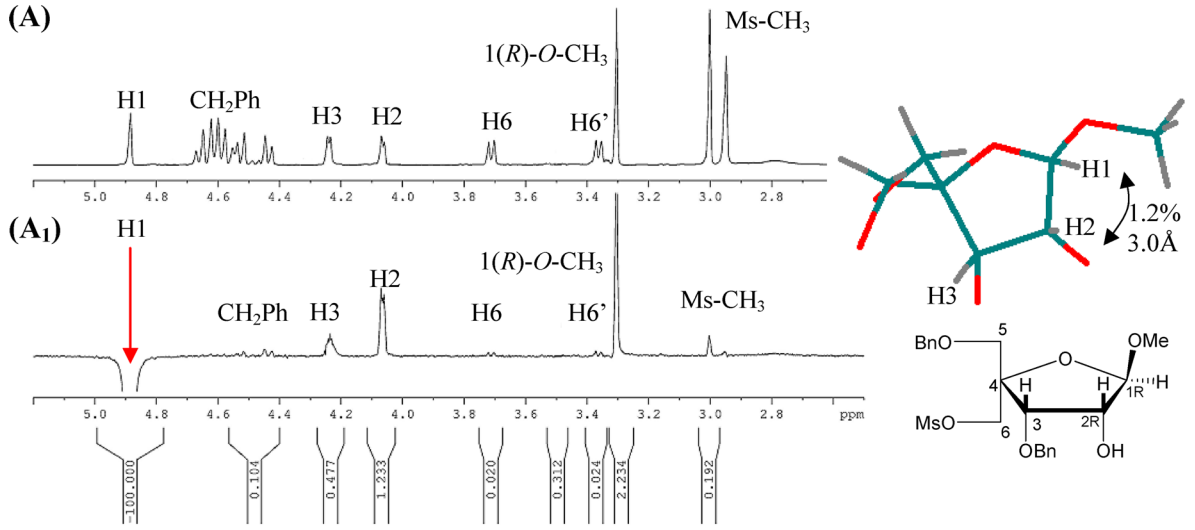

Figure 6. (A) ^{1}H NMR (500 MHz) of compound **12** and (A_1) observed NOE from the irradiation of H1, which shows NOE enhancement with H2 (1.2%, $d_{H7,H2(calc)}$ = 3.0 Å), but a weak NOE with H3 (0.5%, $d_{H1,H3(calc)}$ = 3.9 Å). This suggests that H1 is on the opposite face to H2 and H3, and the configuration of C1 is (*R*).

configuration at the C8 center and (*S*) configuration at the C1 center. Hence, the original assignment of C7(*R*) stereochemistry for compound **4** has remained unchanged during the formation of 5-*exo* bicyclic compound **9** by free-radical reaction.

This confirmation of C7(*R*) stereochemistry was important as an internal reference point for the chirality to confirm the stereochemistry of a new chiral center in compound **9**. Irradiation of 7(*R*)-Me (Figure 5, panel A_3) led to 0.5% NOE enhancement for H8 ($d_{7\text{-Me,H8}} \approx 2.8$ Å), but none for 8(*R*)-Me or H1, and irradiation of H6′ (Figure 5, panel A_4) shows a strong NOE enhancement with H8 (5.4%, $d_{H6,H8} \approx 2.2$ Å), but none for 8-Me. All of these NOE enhancements indicated (*R*) configuration at the C8 center and (*S*) configuration at the C1 center.

Determination of Dihedral Angles through Analysis of 3-Bond $^3J_{HH}$ for (1*S*,2*R*,3*S*,4*R*,7*R*,8*R*)-3-(Benzyloxy)-4-[benzyloxymethyl]-1-[(4-methyloxyphenyl)methoxy]-8,7-dimethylbicyclo[2.2.1]heptane 9. The coupling constants were also used to confirm the configurations of the chiral centers in molecule **9** (Figure S74, Supporting Information part I). The dihedral angles across each bond were calculated through analysis by Karplus equation[21] through the coupling constants input.

The $^3J_{H8,H1}$ of compound **9** is 5 ± 0.2 Hz (Figure S74, panel A_1, in Supporting Information part I), indicating that H1 and H8 have *trans* orientation to each other which corresponds to 8(*R*) configuration. The $^3J_{H2,H3}$ = 4 ± 0.2 Hz (Figure S74, panel A_2, in Supporting Information part I) suggests that the H2 and H3 have *cis* orientation [2(*R*),3(*S*) configuration]. After decoupling of H8, a doublet is observed for H1 with $^3J_{H1,H2}$ = 1.4 ± 0.2 Hz (Figure S73, Supporting Information part I), confirming that H1 and H2 have approximately *cis* orientation, thereby confirming 1(*S*) configuration. Moreover, the $^3J_{H6,H7}$ = 11 ± 0.2 Hz (Figure S74, panel A_3, in Supporting Information part I) indicates a *cis* relationship between H6 and H7 which confirms C7(*R*) configuration.

Synthesis of the Diastereomeric Mixture of (1*R*,2*R*,3*R*,4*R*,7*S*)-3-(Benzyloxy)-4-[(benzyloxy)methyl]-1-[(4-methoxyphenyl)methoxy]-7-methyl-2-oxabicyclo-[2.2.1]heptane (18a) and (1*R*,2*R*,3*R*,4*R*,7*R*)-3-(Benzyloxy)-4-[(benzyloxy)methyl]-1-[(4-methoxyphenyl)methoxy]-7-methyl-2-oxabicyclo[2.2.1]heptane (18b) by the Radical Cyclization Approach. The synthesis of the 3-(benzyloxy)-4-[(benzyloxy)methyl]-1-[(4-methoxyphenyl)methoxy]-7-methyl-2-oxabicyclo[2.2.1]heptanes (**18a**/**18b**) starts from a known intermediate **10**[1d] (Scheme 3), which was converted to the crude 6-*O*-mesylate **11** by the treatment with methanesulfonyl chloride in dry pyridine.[7a]

After workup, the crude 6-*O*-Ms-1,2-*O*-isopropylidene pentose **11** was deprotected with *p*-toluenesulfonic acid·H_2O in methanol to afford compound **12** (92%, over two steps) (Figures S1−S5, Supporting Information part II). Notably, during this methyl glycoside formation step, only one stereoisomer **12**-1(*R*), $[\alpha]_D^{25}$ = −26.9, was obtained. In the NOE where H1 was irradiated (Figure 6, panel A_1), NOE enhancements between H1 with H2 (1.2%, $d_{H1,H2(calc)}$ = 3.0 Å) and H3 (0.5%, $d_{H1,H3(calc)}$ = 3.9 Å) were observed.

This suggests that H1 is on the opposite face of H2 and H3, and the configuration of C1 is (*R*). The $^3J_{H2,H3}$ = 4.8 ± 0.2 Hz (Figure S1, Supporting Information part II) was calculated, which suggests that H2 and H3 are *cisoid* to each other. H1 is a singlet, hence no coupling constant can be measured between H1 and H2. These data prove that the sugar is indeed of *β* configuration, as expected. A suspension of compound **12** and potassium carbonate in MeOH at ∼5 °C afforded the bicyclic 2-oxo-cycloheptane derivative **13** (74%, $[\alpha]_D^{25}$ = −26.3) by overnight stirring. The formation of the new 2-oxo-cycloheptane ring, as in **13**, was evidenced on the basis of the HMBC spectra (Figure S13, Supporting Information part II), where the long-range proton to carbon coupling gave the correlation between C6 and H2 over the 2-oxo substituent.

Overnight hydrolysis of the locked sugar **13** by aqueous *p*-toluenesulfonic acid·H_2O in THF led to **14** with the free formyl ($\delta_{[1\text{-}CH=O]}$ = 9.6 ppm; 90 and 10% hemiacetal, Figure S14, Supporting Information part II). The crude formyl compound **14** was subjected to a Grignard reaction with vinylmagnesium bromide in dry THF overnight to afford the pure alkene diastereomer **15** [C1-(*R*), C4-(*R*)] in 62% yield ($[\alpha]_D^{25}$ = 10.3) after separation. The vinyl resonances at 5.9, 5.4, and 5.2 ppm (Figure S16, Supporting Information part II) in the ^{1}H NMR

dx.doi.org/10.1021/jo300936g | J. Org. Chem. 2012, 77, 6855−6872

spectrum of **15** indicate that the vinyl group is incorporated into the molecule. The configuration at C1 was confirmed by detailed NOE and coupling constant analyses: irradiation of H7 (Figure S22, Supporting Information part II) shows NOE enhancement for H8 (1.6%, $d_{H7,H8(calc)}$ = 2.4 Å), H2 (1.0%, $d_{H7,H2(calc)}$ = 3.1 Å), H3 (0.4%, $d_{H7,H3(calc)}$ = 3.7 Å), and H1 (0.9%, $d_{H7,H1(calc)}$ = 3.1 Å). The key NOE between H8 of the olefin and H3 shows that C1 has an (*R*) configuration, resulting from an α-face attack of the Grignard reagent to 1-CH═O, that is, from the bottom of the 1-CH═O. To further prove the configuration at C1, irradiation of H1 (Figure S21, Supporting Information part II) shows NOE enhancement for H8 (0.9%, $d_{H1,H8(calc)}$ = 3.7 Å) and H2 (1.8%, $d_{H1,H2(calc)}$ = 2.6 Å). These data suggest that H1 is on the opposite face of the alkene. The vicinal coupling constants have been measured, showing $^3J_{H1,H2}$ = 5 ± 0.2 Hz (Figure S25, Supporting Information part II). This means that H1 and H2 are *gauche* to each other, which is also true for H2 and H3 [$^3J_{H2,H3}$ = 3 ± 0.2 Hz] (Figure S23, Supporting Information part II) because they all have the origin from the D-ribose sugar.

The vicinal coupling constant of H1 with H7 (*i.e.*, $^3J_{H1,H7}$ = 5.5 ± 0.2 Hz; Figure S24 in Supporting Information part II) shows that H1 and H7 are *transoid* to each other.

These data suggest that the C1 center has (*R*) configuration, and since the C4 center is part of the locked sugar, the simple hydrolysis step is not likely to alter its (*R*) configuration.

The selective protection of 1-OH with *p*-methoxybenzyl chloride using NaH as a base in dry DMF yielded the olefin **16** [C1-(*R*), C4-(*R*), 71%] ([α]$_D^{25}$ = −25.4). The structure of the olefin **16** has been corroborated by the COSY experiment (Figure S29, panels A,B, in Supporting Information part II), where correlations between H1 and H7, H7 and H8, and H1 and H2 are found. In the long-range proton to carbon correlation experiment (Figure S32, panels A−D, in Supporting Information part II), the following correlations have also been found: H1 and C8, H7/H8 and C1, H8/H1 and C7, and finally H3 and C4, which also corroborate the structural integrity of the olefin **16**. The 1D NOE is shown in Figure S33, Supporting Information part II: irradiation of H7 shows NOE enhancement for H2 (1.3%, $d_{H7,H2(calc)}$ = 3.4 Å) and H1 (1.1%, $d_{H7,H1(calc)}$ = 3.1 Å). In the coupling constant analysis, the following data are found: $^3J_{H1,H2}$ = 3.5 ± 0.2 Hz (Figure S36, panel A_1, in Supporting Information part II). The $^3J_{H1,H2}$ confirms that the relationship between H1 and H2 is *gauche*.

The coupling constant between H1 and H7 is extracted from the ^{1}H decoupling spectrum, where $^3J_{H1,H7}$ = 7.8 ± 0.2 Hz (Figure S35, Supporting Information part II) suggests that H7 (or vinyl-CH) and H1 are *trans*-oriented and the configuration at C1 is confirmed to be (*R*). The olefin **16** in dry pyridine solution was treated with methyl(chlorocarbonyl)formate overnight at 50 °C to give the key free-radical cyclization precursor **17** in good overall yield (73%, [α]$_D^{25}$ = −16.4).

The free-radical cyclization[1d] was carried out under N_2 in anhydrous toluene with Bu_3SnH under reflux, using AIBN as an initiator in a dropwise manner. Cyclization of **17** resulted in an inseparable mixture of diastereomers **18a**/**18b** in moderate yields (47%). The chemical identity and the configurations of **18a**/**18b** have been confirmed by 1D NOEs and detailed coupling constant analysis (Figures S51−S56, Supporting Information part II). Detailed NMR analysis confirms that they both have exclusive β-1-*O*-PMB (C1-*R*) configuration, but they have opposite configurations at C7.

Mechanism of the Formation of the Diastereomeric Mixture of (1*R*,2*R*,3*R*,4*R*,7*S*)-3-(Benzyloxy)-4-[(benzyloxy)methyl]-1-[(4-methoxyphenyl)methoxy]-7-methyl-2-oxabicyclo[2.2.1]heptane (18a) and (1*R*,2*R*,3*R*,4*R*,7*R*)-3-(Benzyloxy)-4-[(benzyloxy)methyl]-1-[(4-methoxyphenyl)methoxy]-7-methyl-2-oxabicyclo-[2.2.1]heptane (18b) from Prop-2-en-1-yl]oxola-3-yl Methyl Oxalate (17). As previously stated, the free-radical ring closure resulted in an intractable mixture of 1,7-*cis*/*trans* diastereomers (1:0.4 by ^{1}H NMR), **18a** (7*S*,1*R*,4*R*) and **18b** (7*R*,1*R*,4*R*). This has been explained by the steric hindrance of the 1-(*R*)-*O*-PMB group which is occupying most of the β-face, and therefore, the 7(*R*)-$CH_2^•$ radical in the β-face is less favored as shown in TS1b and TS2b in panel A of Figure 4. In the Newman projections of **18b** (Figure 4, panel A, arrow b), it is shown that for **18b** there is steric repulsion between the *cis*-oriented 1-(*R*)-*O*-PMB (pseudoaxial) and 7(*R*)-Me (pseudoaxial) in the boat-like transition state (the less favored product). On the other hand, compound **18a** exists in the chair-like transition state, as shown in TS3b and TS4b in panel B in Figure 4, where the steric repulsion is absent between the *trans*-oriented 1-(*R*)-*O*-PMB (pseudoaxial) and 7(*S*)-Me (pseudoequatorial); therefore, **18a** is sterically favorable.

In conclusion, the reaction outcome is affected by the substituent 1-(*R*)-*O*-PMB which occupies the β-face, the H1 and the 7(*S*)-Me are on the α-face, H1 and H7 are *trans* in **18a**, and H1 and H7 are *cis* in compound **18b**. This mechanism therefore suggests that we can engineer the outcome of the ratio of 1,7-*cis*/*trans* diastereomers by controlling the configuration and bulk of the C1 substituent.

NMR Assignments To Support the Structures of Compounds (1*R*,2*R*,3*R*,4*R*,7*S*)-3-(Benzyloxy)-4-[(benzyloxy)methyl]-1-[(4-methoxyphenyl)methoxy]-7-methyl-2-oxabicyclo[2.2.1]heptane (18a) and (1*R*,2*R*,3*R*,4*R*,7*R*)-3-(Benzyloxy)-4-[(benzyloxy)methyl]-1-[(4-methoxyphenyl)methoxy]-7-methyl-2-oxabicyclo-[2.2.1]heptane (18b). In **18a**, the disappearance of the vinyl resonances (at 5.8 and 5.25 ppm) and the O4 oxalyl methyl signal at 3.8 ppm, the chemical shift decrease of H1 (from 3.75 to 3.09 ppm) but also the appearance of the doublet 7-Me at 0.98 ppm suggested that the ring closure had taken place (Figure S43, Supporting Information part II). The formation of the new C4−C7 bond was further evidenced by the correlation between H7−C4 in the HMBC spectrum (Figure S49, panel A, in Supporting Information part II).

The proton to carbon and proton to proton correlations in both HMBC and COSY experiments (Figures S45 and S49, Supporting Information part II) give adequate proof that oxabicyclo[2.2.1]heptane **18a** is indeed formed during the radical cyclization.

In **18b**, the visual appearance of 7-Me and H7 (Figure S43, Supporting Information part II) indicates that this is tentatively the other isomer of the newly formed oxabicyclo[2.2.1]heptane, which is corroborated by the following observations: The H7/7-Me and H1/H7 correlations in the COSY spectrum (Figure S46, panels A,B, in Supporting Information part II). In the HMBC experiment (Figure S50, panel C, in Supporting Information part II), it is seen that H7 and C4 are long-range coupled, this confirms that the ring closure has taken place.

Determination of Configuration through NOE Analysis and the Determination of Dihedral Angles through Analysis of 3-Bond $^3J_{HH}$ of Compounds 3-(Benzyloxy)-4-[(benzyloxy)methyl]-1-[(4-methoxyphenyl)methoxy]-7-methyl-2-oxabicyclo[2.2.1]heptanes 18a/18b. The orientation of the substituents (at C1 and C7) in the carbocyclic

dx.doi.org/10.1021/jo300936g | J. Org. Chem. 2012, 77, 6855−6872

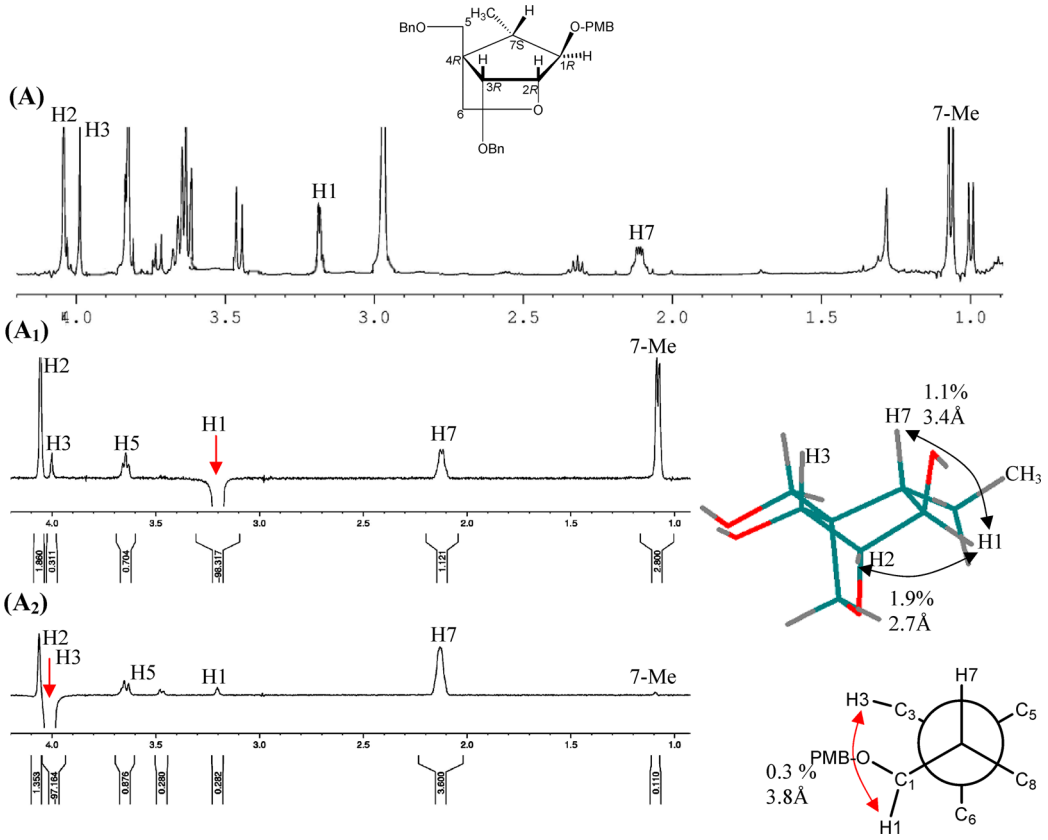

Figure 7. (A) ^{1}H NMR (500 MHz) of compound **18a**. (A_1) NOE spectrum where irradiation of H1 shows strong NOE enhancement with CH_3 and H2. (A_2) NOE where irradiation of H3 again proves that H3 and H7 are on the β-face. These data show that H1 and H7 are on the opposite faces and are *trans*. H1 and CH_3 are on the α-face, C1 is of (*R*) configuration, and C7 is of (*S*) configuration.

skeleton of compounds **18a**/**18b** was determined by 1D NOE experiments (Figures 7 and 8) as well as from the vicinal coupling constant evaluations.

For compound **18a**, irradiation of H1 (Figure 7, panel A_1) shows NOE enhancement for 7(*S*)-CH_3 (2.8%, $d_{H1,7\text{-}Me(calc)}$ = 2.8 Å), H7 (1.1%, $d_{H1,H7(calc)}$ = 3.4 Å), H3 (0.3%, $d_{H1,H3(calc)}$ = 3.8 Å), and H2 (1.9%, $d_{H1,H2(calc)}$ = 2.7 Å). This indicates that H1 has the same orientation as 7-Me, but not H3, which shows that the stereochemistry of C1 is of (*R*) configuration.

In a similar way, irradiation of H7 (Figure S53, Supporting Information part II) shows NOE enhancement for 7(*S*)-Me (2.7%, $d_{H7,7\text{-}Me(calc)}$ = 3.2 Å), H1 (1.3%, $d_{H7,H1(calc)}$ = 3.4 Å), H6 (1.2 and 0.8%), H3 (3.7%, $d_{H7,H3(calc)}$ = 2.5 Å), and H2 (0.2%, $d_{H7,H2(calc)}$ = 4.3 Å), which proves that H7 and H3 are on the β-face. To further verify the configuration of C1 and C7, irradiation of H3 (Figure 7, panel A_2) was performed which showed enhancement for 7(*S*)-Me (0.1%, $d_{H3,7\text{-}Me(calc)}$ = 4.3 Å), H7 (3.6%, $d_{H3,7\text{-}Me(calc)}$ = 2.2 Å), H1 (0.3%, $d_{H3,H1(calc)}$ = 3.8 Å), and H2 (1.4%, $d_{H3,H2(calc)}$ = 2.8 Å). These suggest that H1 and H7 are *trans*-oriented.

On the other hand, the homonuclear ^{1}H decoupling of H2 shows that H1 is coupled to H7 with a $^3J_{H1,H7}$ = 3 ± 0.2 Hz (Figure S58, Supporting Information part II), which indicates that H1 and H7 are in *trans* relationship with each other. ^{1}H decoupling of H7 (Figure S59, Supporting Information part II) turned H1 into a singlet, which proves that there is no coupling observed between H1 and H2. The broad singlets of H2 and H3 indicate that these protons have too small coupling to each other and no coupling can be measured between H2 and H3.

In compound **18b**, irradiation of H7 (Figure 8, panel A_2) shows NOE enhancement for H1 (9.5%, $d_{H7,H1(calc)}$ = 2.3 Å), which suggests that H1 and H7 are on the same face (α-face). Irradiation of 7(*R*)-Me (Figure 8, panel A_1) shows NOE enhancement for H1 (1.7%, $d_{7\text{-}Me,H1(calc)}$ = 3.3 Å), H3 (1.6%, $d_{7\text{-}Me,H3(calc)}$ = 3 Å), and H2 (0.6%, $d_{7\text{-}Me,H2(calc)}$ = 4.3 Å). This proves that 7(*R*)-Me and H3 are both on the β-face, which suggests that H1 and H7 are *cis*-oriented.

^{1}H decoupling experiment of H7 (Figure S60, Supporting Information part II) shows that 7-Me is affected, but since H1 is a multiplet and it overlaps with H6, the coupling from H1 cannot be calculated. However, ^{1}H decoupling of 7-Me gives the $^3J_{H1,H7}$ = 8 ± 0.2 Hz (Figure S61, Supporting Information part II) which proves that H1 and H7 are *cis* to each other.

Steric-Dependent Origin of Different Stereochemical Outcome. *What Is the Difference in the Outcome of the Grignard Reaction with the Carba-Ring (**5**→**6**) in the α-Face Compared to That of the Furano Ring (**14**→**15**)?* The outcome of the Grignard reaction on the formyl/hemiacetal group of the furanose system (**5** → **6** in Scheme 2) to give the alkene-diol **6** (1*S*,1*R* mixture) is affected by the steric clash of the 7(*R*)-Me and the Grignard reagent in the α-face of the 2,4-carba-ring. Hence, the β-attack by the Grignard reagent from the "top face" is favored in **5** → **6**, which is fully supported by the NOE (particularly NOE between H1 and H3; see Table S1, Supporting Information part I). In contradistinction, the same reaction on the formyl **14** (**14** → **15** in Scheme 3) giving alkene-diol **15** with the 2-*O* of the furane ring in the α-face resulted in an α-attack from the α-face with (*R*) configuration at C1 exclusively because, given that the substituents on the β-face in **5** and **14** are

dx.doi.org/10.1021/jo300936g | J. Org. Chem. 2012, 77, 6855−6872

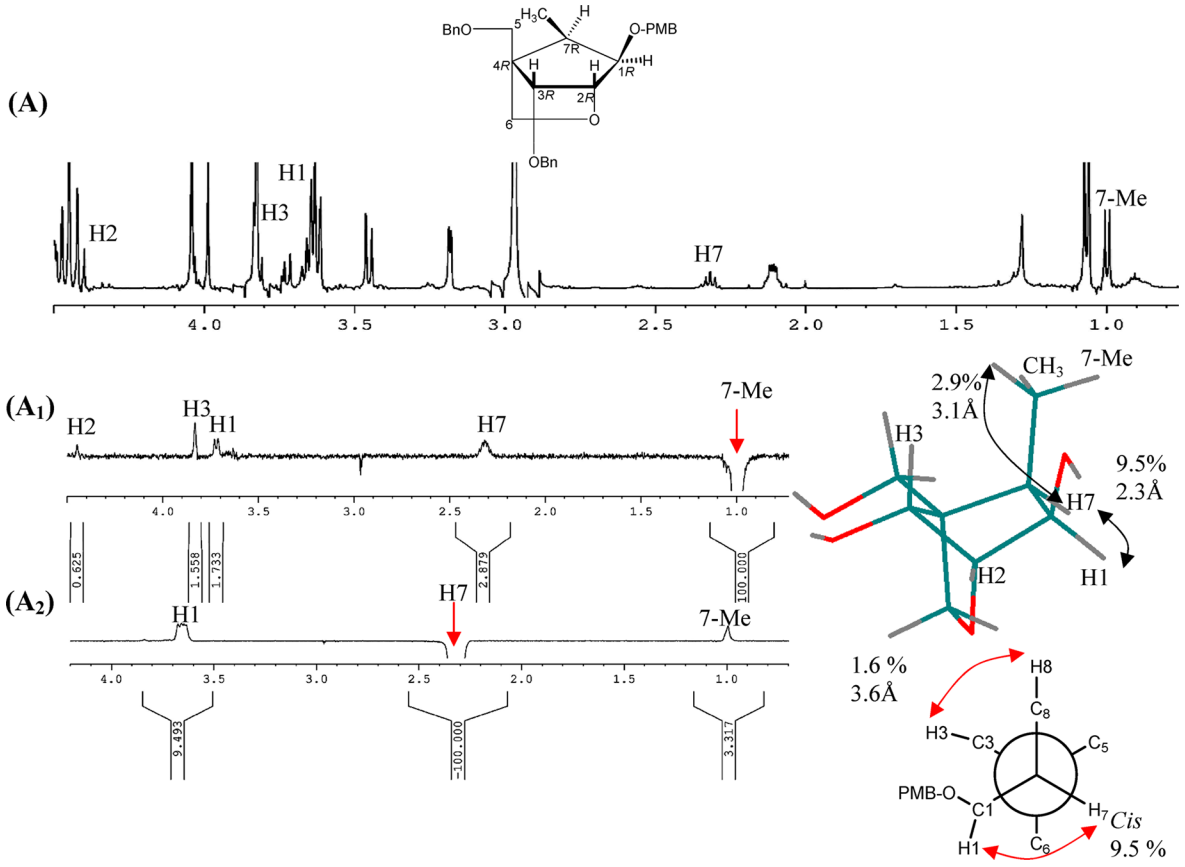

Figure 8. (A) ^{1}H NMR (500 MHz) of compound **18b**. (A_1) NOE where irradiation of H7 suggests that H1 and H7 are *cis*. (B) ^{1}H NMR (500 MHz) of compound **18b**. (A_2) NOE where irradiation of H8 suggests that CH_3 and H3 are on the β-face of the fused oxabicyclo[2.2.1]heptane (**18b**). These data show that both C1 and C7 have (*R*) configuration.

identical, the furano-oxygen in **14** has been assumed to form a Lewis acid−base complex[16a−c] with vinylmagnesium bromide, thereby enabling the vinyl group to add to the aldehyde from the α-face.

*What Is the Difference in the Outcome of the Free-Radical Cyclization Giving 2,5-Dimethylbicyclo[2.2.1]heptane (**8** →**9**) Compared to 7-Methyl-2-oxabicyclo[2.2.1]heptane (**17**→ **18a/18b**)?* Taking into consideration that the radical cyclization generally proceeds via a boat- and a chair-like transition state, we have shown that our two different chiral carba systems, one with 2,4-carba bridge **8** in the α-face and **17** with 2-*O* of the furane ring in the α-face, proceed with different stereoselectivity. This is due to the steric factors that control the stereochemistry of the radical cyclization from precursors **8** and **17** to give the new C4−C8 bond in **9** (Scheme 2) and C4−C7 bond in **18a** and **18b**, respectively (Scheme 3).

In the ring closure of **8**, the only product obtained is the 2,5-dimethylbicyclo[2.2.1]heptane (**9**). The transition state is a boat-like transition state resulting in the 1,8-*trans* product exclusively, and this is due to the steric clash of the bulky 1(*S*)-*O*-*p*-methoxybenzyl (PMB) and 7(*R*)-Me in the α-face (pseudoequatorial orientations, Figure 4, TS1a and TS2a in panel A). In contrast, the ring closure of **17** (Scheme 3) resulted in a diastereomeric mixture of 1(*R*)-7-methyl-2-oxabicyclo[2.2.1]-heptanes (**18a**/**18b**, 6:4), which was intractable and could not be separated. Both the boat- and the chair-like transition states are possible: the latter resulted in the major 1,7-*trans* product observed. The 1,7-*cis* product [between the 1(*R*)-*O*-PMB and 7(*R*)-Me] was formed as a minor product because of the steric hindrance by the 1(*R*)-*O*-PMB group (TS1b and TS2b, panel A in Figure 4), which is arising from the boat-like conformation, which was competing with the chair-like transition state (TS3b and TS4b, panel B in Figure 4).

*Determination of Dihedral Angles through Analysis of 3-Bond $^3J_{HH}$ by Karplus Equation for **9** versus **18a/18b** and the Newman Projection.* In compound **9** (the sole isomer in which H8/C5 are *transoid*), the Newman projections across the C1−C8 (projection A_1), C4−C6 (projection A_2), and C7−C2 (projection A_3) bonds are shown (Figure 9, panel A). The experimentally derived $^3J_{H1,H8} = 5 \pm 0.2$ Hz gives the dihedral angle for the corresponding torsion, $\phi_{H1-C8-C8-H8} = 132 \pm 2°$, as can be found in projection A_1; with these torsion angles fixed, we could then calculate the other significant torsions through modeling in HyperChem (MM/Amber and semiempirical/AM1) which in turn shows through projection A_2 that the $\phi_{8\text{-Me}-C8-C4-C5} = 37 \pm 2°$, $\phi_{8\text{-Me}-C8-C4-C6} = 165 \pm 2°$, and $\phi_{8\text{-Me}-C8-C4-C3} = 89 \pm 2°$, thereby showing that the chirality of the C4 center has remained unchanged. The Newman projection A_3 across the C7−C2 shows experimental $^3J_{H2,H7} = 5.4 \pm 0.2$ Hz, giving torsion, $\phi_{H2-C2-C7-H7} = 46 \pm 2°$, which is further discussed in the legend of Figure 9.

The Newman projections across the C8−C4 (B_1), C3−C2 (B_2), and C7−C6 (B_3) bonds are shown in Figure 9. Projection B_2 through C3−C2 shows an experimental $^3J_{H2,H3} = 4 \pm 0.2$ Hz, giving torsion, $\phi_{H2-C2-C3-H3} = 60 \pm 2°$, which is fully explained by the legend of Figure 9: note that these torsions could be easily obtained because we have a [2.2.1]-fused cycloheptane system

dx.doi.org/10.1021/jo300936g | J. Org. Chem. 2012, 77, 6855−6872

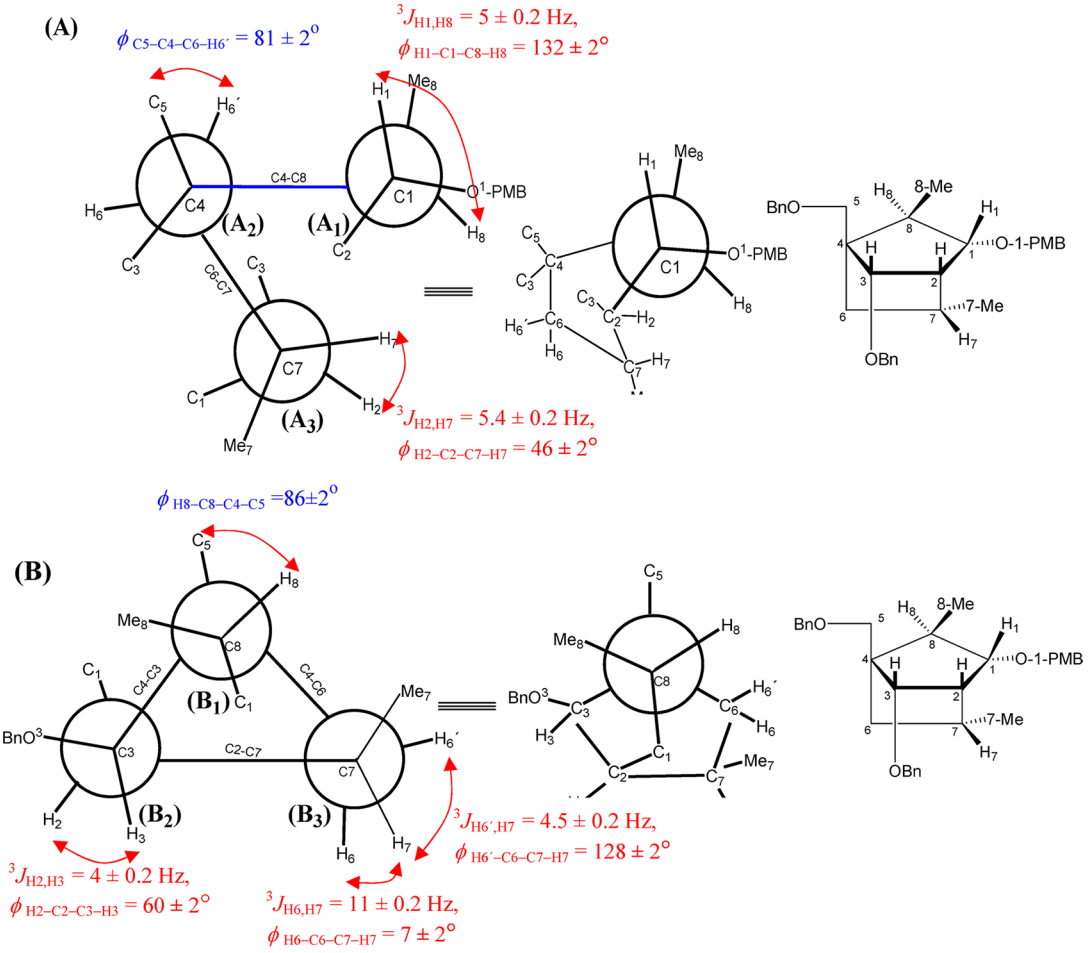

Figure 9. (A) Newman projection across the C1−C8 (A_1), C4−C6 (A_2), and C7−C2 (A_3) bonds in dimethylbicyclo[2.2.1]heptane **9**. Projection A_1 through C1−C8 bond shows an experimental $^3J_{H1,H8} = 5 \pm 0.2$ Hz, giving torsion, $\phi_{H1-C1-C8-H8} = 132 \pm 2°$, which in turn shows through projection A_2 that the $\phi_{8\text{-Me}-C8-C4-C5} = 37 \pm 2°$, $\phi_{8\text{-Me}-C8-C4-C6} = 165 \pm 2°$, and $\phi_{8\text{-Me}-C8-C4-C3} = 89 \pm 2°$, thereby showing that the chirality of the C4 center has remained unchanged. Projection A_3 through C7−C2 bond shows experimental $^3J_{H2,H7} = 5.4 \pm 0.2$ Hz, giving torsion, $\phi_{H2-C2-C7-H7} = 46 \pm 2°$, which in turn shows that the $\phi_{H7-C7-C2-C1} = 178 \pm 2°$ and $\phi_{H7-C7-C2-C3} = 78 \pm 2°$. (B) Newman projections through the C8−C4 (B_1), C3−C2 (B_2), and C7−C6 (B_3) bonds in compound **9**. Projection B_2 through C3−C2 bond shows an experimental $^3J_{H2,H3} = 4 \pm 0.2$ Hz, giving torsion, $\phi_{H2-C2-C3-H3} = 60 \pm 2°$, thereby showing through projection B_2 that the $\phi_{H2-C2-C3-OBn} = 58 \pm 2°$, $\phi_{C1-C2-C3-OBn} = 179 \pm 2°$ and $\phi_{C5-C4-C8-H8} = 86 \pm 2°$ in projection B_1. Experimental $^3J_{H6,H7} = 11 \pm 0.2$ Hz corresponds to $\phi_{H6-C6-C7-H7} = 7 \pm 2°$, and $^3J_{H6',H7} = 4.5 \pm 0.2$ Hz corresponds to $\phi_{H6'-C6'-C7-H7} = 128 \pm 2°$, thereby showing through projection B_3 that the $\phi_{H6-C6-C7-7\text{-Me}} = 113 \pm 2°$, $\phi_{H6'-C6-C7-7\text{-Me}} = 8 \pm 2°$.

with a bridgehead at C4. So that also settles the configuration of C4 to be (*R*), which, as expected, has remained unchanged.

On the other hand, for compound **18a** (the major isomer in which H7/C5 are *cisoid*), the Newman projection across the C1−C7 (A_1) and C4−C6 (A_2) bonds are shown in Figure 10. The experimentally derived $^3J_{H1,H7}$ of 3 ± 0.2 Hz (in projection A_1) gives the dihedral angle for the corresponding torsion, $\phi_{H1-C1-C7-H7}$ of 123 ± 2°, and with this torsion angle fixed, we could then calculate the other significant torsions through modeling in HyperChem. Projection A_1 shows that the $\phi_{H7-C7-C1-O\text{-PMB}} = 3 \pm 2°$, $\phi_{O1\text{-PMB}-C1-C7-7\text{-Me}} = 117 \pm 2°$, $\phi_{H1-C1-C7-7\text{-Me}} = 3 \pm 2°$, $\phi_{H1-C1-C7-C4} = 117 \pm 2°$, $\phi_{C4-C7-C1-C2} = 3 \pm 2°$, and $\phi_{C2-C1-C7-H7} = 112 \pm 2°$. The bonds in projection A_2 are fully explained in the legend of Figure 10. The configuration at C4 has remained as (*R*). For compound **18b** (the minor isomer in which H7/C5 are *transoid*), the Newman projections across the C1−C7 (B_1) and C4−C6 (B_2) bonds are shown in Figure 10. Panel B_1 shows the experimentally derived $^3J_{H1,H7}$ of 8 ± 0.2 Hz, $\phi_{H1-C1-C7-H7}$ of 3 ± 2°, and with this torsion angle fixed, we could then calculate the other significant torsions through modeling in HyperChem, which in turn shows through projection B_1 that the $\phi_{H7-C7-C1-O\text{-PMB}} = 129 \pm 2°$, $\phi_{O\text{-PMB}-C1-C7-7\text{-Me}} = 7 \pm 2°$, $\phi_{7\text{-Me}-C7-C1-C2} = 123 \pm 2°$, $\phi_{H1-C1-C7-C4} = 118 \pm 2°$, $\phi_{7\text{-Me}-C7-C4-C5} = 42 \pm 2°$, $\phi_{7\text{-Me}-C7-C4-C3} = 86 \pm 2°$, and $\phi_{7\text{-Me}-C7-C4-C6} = 170 \pm 2°$. For projection B_2 details, see caption of Figure 10. These show that the chirality of C4 center has remained unchanged. The significant torsions were obtained because the 2-oxo-[2.2.1]-fused cycloheptane system has a bridgehead at C4, so configuration of C4 has to be (*R*).

■ CONCLUSIONS

In this study, we have synthesized dimethylbicyclo[2.2.1]-heptane (**9**) stereospecifically and a diastereomeric mixture of 7-methyl-2-oxabicyclo[2.2.1]heptanes (**18a**/**18b**, 6:4) by the free-radical ring-closure reaction approach. We have speculated that the outcome of the reaction is controlled by the stereochemical environments around the new radical addition center, C4 and C8−C9 olefin in the radical precursor **8** to give **9** and C4 and C7−C8 olefin in **17** to give **18a**/**18b**. The role of

dx.doi.org/10.1021/jo300936g | J. Org. Chem. 2012, 77, 6855−6872

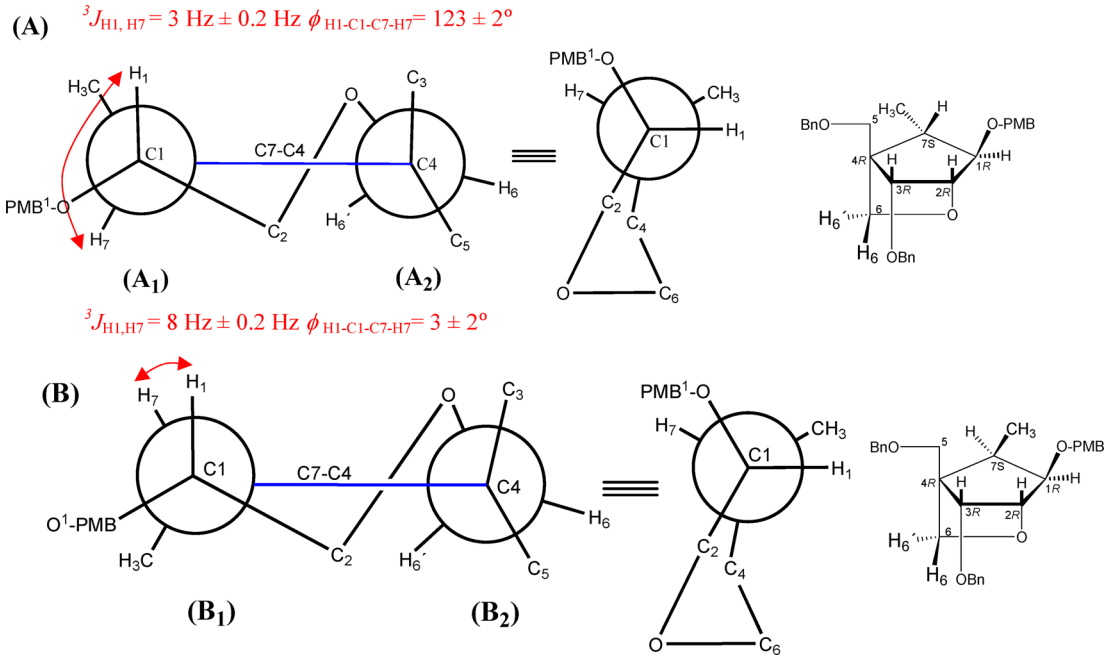

Figure 10. (A) Newman projection through the C1−C7 (A_1) and C4−C6 (C_2) bonds in compound **18a**. (A_1) Experimental $^3J_{H1,H7}$ of 3 ± 0.2 Hz, giving torsion $\phi_{H1-C1-C7-H7}$ = 123 ± 2°, which in turn shows through projection A_1 that the $\phi_{H7-C7-C1-O\text{-}PMB}$ = 3 ± 2°, $\phi_{O\text{-}PMB-C1-C7-7\text{-}Me}$ = 117 ± 2°, $\phi_{H1-C1-C7-7\text{-}Me}$ = 3 ± 2°, $\phi_{H1-C1-C7-C4}$ = 117 ± 2°, $\phi_{C4-C7-C1-C2}$ = 3 ± 2°, $\phi_{C2-C1-C7-H7}$ = 112 ± 2°, thereby showing through projection C_2, $\phi_{C3-C4-C6-H6}$ = 80 ± 2°, $\phi_{C5-C4-C6-H6}$ = 48 ± 2°, $\phi_{C5-C4-C6-H6'}$ = 78 ± 2°, $\phi_{H6'-C6-C4-C7}$ = 50 ± 2°, $\phi_{C7-C4-C6-O2}$ = 73 ± 2°, $\phi_{O2-C6-C4-C3}$ = 36 ± 2°, and $\phi_{7\text{-}Me-C7-C4-C6}$ = 58 ± 2°. (B) Newman projection of compound **18b** through the C1−C7 (B_1) and C4−C6 (B_2) bonds. (B_1) Experimental $^3J_{H1,H7}$ of 8 ± 0.2 Hz, $\phi_{H1-C1-C7-H7}$ of 3 ± 2°, which in turn shows through projection B_1 that the $\phi_{H7-C7-C1-O\text{-}PMB}$ = 129 ± 2°, $\phi_{O\text{-}PMB-C1-C7-7\text{-}Me}$ = 7 ± 2°, $\phi_{7\text{-}Me\ -C7-C1-C2}$ = 123 ± 2°, $\phi_{H1-C1-C7-C4}$ = 118 ± 2°, $\phi_{7\text{-}Me-C7-C4-C5}$ = 42 ± 2°, and $\phi_{7\text{-}Me\ -C7-C4-C6}$ = 170 ± 2°, which in turn shows through projection B_2 that $\phi_{C7-C4-C6-O2}$ = 71 ± 2°, $\phi_{O2-C6-C4-C3}$ = 36 ± 2°, $\phi_{C3-C4-C6-H6}$ = 80 ± 2°, $\phi_{H6-C6-C4-C5}$ = 48 ± 2°, $\phi_{C5-C4-C6-H6'}$ = 79 ± 2°, $\phi_{H6'-C6-C4-C7}$ = 48 ± 2°. Taken these torsions together, it can be found that the chirality of C4 center has remained unchanged.

steric factors for different chair- and the boat-like transitions states have been evaluated.

In the free-radical cyclization of **8**, the single product observed is the 2,5-dimethylbicyclo[2.2.1]heptane (**9**) because the transition state adopts a boat-like conformation which resulted in the 1,8-*trans* product (favored) due to the *absence* of steric clash of the bulky 1(*S*)-*O*-*p*-methoxybenzyl (PMB) and 7(*R*)-Me with 8(*R*)-$CH_2^\bullet$ radical (TS1a and TS2a in Figure 4) in the *α*-face, giving an outcome of one pure bicyclo[2.2.1]heptane **9**. On the other hand, the ring closure of **17** resulted in a diastereomeric mixture of 1(*R*)-7-methyl-2-oxabicyclo[2.2.1]heptanes (**18a**/**18b**, 6:4) because both boat-like (TS1b and TS2b in Figure 4) and the chair-like (TS3b and TS4b in Figure 4) transition states with low energy barrier are possible. The chair-like transition state gives the major 1,7-*trans* addition product. On the other hand, the minor 1,7-*cis* product is formed because of the steric clash between the 1(*R*)-*O*-PMB and 7(*R*)-Me.

Various 1D NMR experiments, including ^{1}H, ^{13}C, ^{1}H homodecoupling experiments, 1D nuclear Overhauser effect spectroscopy (1D NOE), 2D COSY, one-bond ^{1}H−^{13}C correlation (HMQC), and long-range ^{1}H−^{13}C HMBC correlation have been employed to characterize the synthesized compounds unambiguously.

The configurations of the substituents of the key intermediates as well as that of the final compounds have been determined by 1D NOE and the dihedral angles determined through analysis of 3-bond $^3J_{HH}$ (experimentally derived) by Karplus equation. The molecular structures have been studied by MM and semi-empirical simulations in HyperChem to understand the stereochemistry of the key intermediates and the cyclization products.

Implications. Work is in progress to exploit this new chemistry and the products for synthesis of modified oligonucleotides in order to explore their biological activity. The stereochemical outcome is rationalized by the steric factors, and having grasped this information, we believe that we are in a position to predict successfully the stereochemistry at the centers of the newly formed C−C bond by modifying the bulkiness of the substituents around the sugar moiety. With less rigid conformations and less bulky substituents around the radical center, several isomers are likely to be formed. In contradistinction, with more rigid conformationally constrained conformations and bulkier substituents around the radical center, only one product may be obtained in a stereospecific manner. This opens new possibilities for the syntheses of novel chiral carba- or double carba-LNAs through the free-radical ring-closure reaction with a *transient* conformationally constrained group at the radical center, which can be removed at the end of the free-radical ring-closure reaction. These transient groups may include bifunctional cyclic reagents, such as tetraisopropyldisiloxane-1,3-diyl,[17] tetraisopropyldisiloxane,[18] isopropylidene[19]).

EXPERIMENTAL SECTION

General Procedures. All reagents were the highest commercial quality and were used without further purification. All nonaqueous reactions were carried out under anhydrous conditions in dry, freshly distilled solvents under N_2(g). Reactions were monitored by TLC carried out using UV light as visualizing agent and/or cerium ammonium molybdate. Flash chromatography was performed using silica gel 60 (230−400 mesh). ^{1}H, ^{13}C NMR were obtained using 500 and 600 MHz instruments for ^{1}H and 125 and 150 MHz for ^{13}C. The same spectrometers were used for the acquisition of ^{1}H−^{1}H

dx.doi.org/10.1021/jo300936g | J. Org. Chem. 2012, 77, 6855−6872

homonuclear (COSY and NOE) and $^{1}H-^{13}C$ heteronuclear (HSQC and HMBC) correlations. Optical rotations were recorded on a polarimeter, and values are reported as follows: $[\alpha]_{\lambda}^{T}$ (c (g/100 mL), solvent). The molecular modelings have been performed using HyperChem Pro 6.0[20] using MM (AMBER) followed by semiempirical (AM1) method (as implemented in HyperChem Pro. 6.0) to analyze the structures of all products reported in the schemes. The dihedral angles have been obtained using Karplus equation[21a,b] through the coupling constant (NMR data) input, whereas HyperChem was used where no coupling constant could be obtained. High-resolution mass spectra (HRMS) with correct masses have been obtained by MALDI-TOF mass spectroscopy.

4-*C*-Allyl-3,5-di-*O*-benzyl-1-*O*-methyl-α,β-D-ribofuranoside (2). Compound **1** (1 g, 2.44 mmol) was stirred with 6% *p*-toluenesulfonic acid·H_2O in MeOH (15 mL) at rt for 24 h; the mixture was neutralized with saturated solution of $NaHCO_3$, concentrated, diluted with H_2O, and extracted with CH_2Cl_2. After drying over $MgSO_4$, it was purified by silica gel column chromatography (EtOAc/petroleum ether 1/5−2/5) to give compound **2** as a colorless oil (800 mg, 86%) as an inseparable mixture of anomer α:β.

Major Isomer: ^{1}H NMR (600 MHz, $CDCl_3$) δ 7.28−7.38 (13H, m, aromatic), 5.95 (1H, m, H7), 5.12 (2H, m, H8, H8′), 4.86 (1H, s, H1), 4.69 (1H, d, J_{gem} = 12 Hz, C$\underline{H}_2$Ph), 4.61 (1H, d, J_{gem} = 12 Hz, C$\underline{H}_2$Ph), 4.56 (2H, s, C$\underline{H}_2$Ph), 4.16 (1H, d, $J_{3,2}$ = 5.4 Hz, H3), 4.08 (1H, dd, $J_{2,1}$ = 3 Hz, $J_{3,2}$ = 5.4 Hz, H2), 3.55 (1H, d, J_{gem} = 9 Hz, H5), 3.28 (1H, d, J_{gem}= 9 Hz, H5′), 3.31 (3H, s, OC$\underline{H}_3$), 2.55 (2H, d, J_{gem} = 7.2 Hz, H6, H6′); ^{13}C NMR (150 MHz, $CDCl_3$) δ 138.7, 138.5 (aromatic), 134.4 (C7), 128.9, 128.4, 128.2, 127.9 (aromatic), 118.3 (C8), 107.6 (C1), 86.8 (C4), 82.1 (C2), 75.2 (C5), 75.1 (C3), 73.3 (C$\underline{H}_2$Ph), 72.8 (C$\underline{H}_2$Ph), 55.3 (O$\underline{C}H_3$), 38.1 (C6); MALDI-TOF m/z $[M + Na]^+$ calcd for $C_{23}H_{28}NaO_5$ 407.183, found 407.186.

4-*C*-Allyl-3,5-di-*O*-benzyl-1-*O*-methyl-2-*O*-phenoxythiocarbonyl-β-D-ribofuranoside (3a), 4-*C*-Allyl-3,5-di-*O*-benzyl-1-*O*-methyl-2-*O*-phenoxythiocarbonyl-α-D-ribofuranoside (3b). Compound **2** (5 g, 13.01 mmol) was dissolved in 100 mL of anhydrous pyridine. The solution was cooled to 0 °C, and then phenyl chlorothionoformate was added dropwise (3.53 mL, 26.02 mmol), while temperature was maintained at 0 °C during the addition. After overnight stirring at room temperature, pyridine was recovered under reduced pressure. The residue was dissolved in CH_2Cl_2 and washed with saturated solution of $NaHCO_3$ twice. The organic layer was separated, dried over $MgSO_4$, and concentrated. The concentrate was purified by silica gel column chromatography (0−10% EtOAc in petroleum ether, v/v) to give compound **3** as a yellowish oil (6 g, 88%) as a separable mixture of anomers α (**3b**, 22%), β (**3a**, 66%).

Anomer β: ^{1}H NMR (500 MHz, $CDCl_3$) δ 7.13−7.26 (13H, m, aromatic), 6.90 (2H, d, J = 8.5 Hz, aromatic), 5.82 (1H, m, H7), 5.63 (1H, d, $J_{2,3}$ = 5 Hz, H2), 5.01 (1H, d, $J_{1,2}$ = 3 Hz, H1), 4.98 (2H, d, $J_{8,8'}$ = 3 Hz, H8, H8′), 4.54 (2H, s, C$\underline{H}_2$Ph), 4.49 (1H, d, J_{gem} = 11.5 Hz, C$\underline{H}_2$Ph), 4.41 (1H, d, J_{gem} = 11.5 Hz, C$\underline{H}_2$Ph), 4.35 (1H, d, $J_{3,2}$ = 5 Hz, H3), 3.46 (1H, d, J_{gem} = 9 Hz, H5), 3.27 (1H, d, J_{gem} = 9 Hz, H5′), 3.26 (3H, s, OC$\underline{H}_3$), 2.39 (2H, m, H6, H6′); ^{13}C NMR (125 MHz, $CDCl_3$) δ 194.4 (C═S), 153.3, 151.0, 138.3, 137.9 (aromatic), 133.9 (C7), 128.3, 127.5, 126.8, 121.9, 120.9 (aromatic), 117.9 (C1), 104.4 (C8), 85.1 (C4), 84.2 (C2), 79.4 (C3), 73.9 (C5), 73.3 (C$\underline{H}_2$Ph), 73.4 (C$\underline{H}_2$Ph), 55.1 (O$\underline{C}H_3$), 37.4 (C6); MALDI-TOF m/z $[M + Na]^+$ calcd for $C_{30}H_{32}NaO_6S$ 543.182, found 543.180.

Anomer α: ^{1}H NMR (600 MHz, $CDCl_3$) δ 7.19−7.35 (13H, m, aromatic), 6.98 (2H, d, J = 7.8 Hz, aromatic), 5.80 (1H, m, H7), 5.43 (1H, dd, $J_{2,3}$ = 6 Hz, $J_{2,1}$ = 4.8 Hz, H2), 5.15 (1H, d, $J_{1,2}$ = 4.8 Hz, H1), 4.94 (2H, m, H8, H8′), 4.61 (1H, d, J_{gem} = 12 Hz, C$\underline{H}_2$Ph), 4.47 (1H, d, J_{gem} = 12 Hz, C$\underline{H}_2$Ph), 4.49 (1H, d, J_{gem} = 12 Hz, C$\underline{H}_2$Ph), 4.33 (1H, d, J_{gem} = 12 Hz, C$\underline{H}_2$Ph), 4.29 (1H, d, $J_{3,2}$ = 4.8 Hz, H3), 3.42 (3H, s, OC$\underline{H}_3$), 3.2 (1H, d, J_{gem} = 9.6 Hz, H5), 3.27 (1H, d, J_{gem} = 9.6 Hz, H5′), 2.68 (1H, dd, J_{gem} = 14.4 Hz, $J_{6,7}$ = 6 Hz, H6); ^{13}C NMR (150 MHz) δ 195.21 (C═S), 153.9 (aromatic), 134.4 (C7), 129.0, 128.1, 128.0, 126.5, 122.2 (aromatic), 118.3 (C8), 101.7 (C1), 86.9 (C4), 79.7 (C2), 77.6 (C3), 74.9 (C$\underline{H}_2$Ph), 73.9 (C$\underline{H}_2$Ph), 73.6 (C5), 55.3 (O$\underline{C}H_3$), 38.4 (C6); MALDI-TOF m/z $[M + Na]^+$, calcd for $C_{30}H_{32}NaO_6S$ 543.182, found 543.183.

(1*R*,3*S*,4*R*,7*R*)-3-Benzyloxy-5-benzyloxymethyl-1-methoxy-7-methyl-8-oxa-bicyclo[2.2.1]heptane (4a) and (1*R*,3*S*,4*R*,7*S*)-3-Benzyloxy-5-benzyloxymethyl-1-methoxy-7-methyl-8-oxa-bicyclo[2.2.1]heptane (4b). Compound **3** (2 g, 3.73 mmol) was dissolved in 80 mL of anhydrous toluene to which N_2 was purged for 30 min. The mixture was heated to reflux, and Bn_3SnH (2.01 mL in 10 mL anhydrous toluene) and AIBN (0.31 g in 10 mL anhydrous toluene) were added dropwise in 2 h and reflux was continued for 2 h. Solvent was evaporated, and the concentrate was purified by silica gel column chromatography (0−10% EtOAc in petroleum ether, v/v) to give 0.9 g of diastereomeric mixture of two isomers **4a** and **4b** as a colorless oil (60%) in 3:1 ratio, respectively. The major isomer **4a** was isolated but the minor isomer **4b** contained a 30% impurity of **4a**.

4a: ^{1}H NMR (500 MHz, $CDCl_3$) δ 7.18−7.26 (10H, m, aromatic), 4.77 (1H, s, H1), 4.54 (1H, d, J_{gem} = 12 Hz, C$\underline{H}_2$Ph), 4.52 (1H, d, J_{gem} = 12 Hz, C$\underline{H}_2$Ph), 4.41 (1H, d, J_{gem} = 11.5 Hz, C$\underline{H}_2$Ph), 4.44 (1H, d, J_{gem} = 11.5 Hz, C$\underline{H}_2$Ph), 4.14 (1H, s, H3), 3.58 (1H, d, J_{gem} = 11 Hz, H5′), 3.55 (1H, d, J_{gem} = 11 Hz, H5), 3.30 (3H, s, OC$\underline{H}_3$), 2.37 (1H, m, H7), 2.22 (1H, d, $J_{2,3}$ = 3 Hz, H2), 1.94 (1H, dd, J_{gem} = 11 Hz, $J_{6,7}$ = 3.7 Hz, H6), 1.12 (1H, dd, J_{gem} = 11 Hz, $J_{6,7}$ = 3.7 Hz, H6), 1.02 (3H, d, J = 9 Hz, C$\underline{H}_3$); ^{13}C NMR (125 MHz) δ 138.6, 138.4 (aromatic), 129.6, 128.3, 127.6, 127.4, 127.3 (aromatic), 101.7 (C1), 87.1 (C4), 82.9 (C3), 73.5 (C$\underline{H}_2$Ph), 71.7 (C$\underline{H}_2$Ph), 69.2 (C5), 54.7 (O$\underline{C}H_3$), 48.7 (C2), 37.6 (C6), 27.9 (C7), 15.9 (C$\underline{H}_3$); MALDI-TOF m/z $[M + Na]^+$ calcd for $C_{23}H_{28}NaO_4$ 391.189, found 391.188.

4b: ^{1}H NMR (500 MHz, $CDCl_3$) δ 7.24−7.34 (14H, m, aromatic), 4.56 (1H, s, H1), 4.67 (1H, d, J_{gem} = 12 Hz, C$\underline{H}_2$Ph), 4.61 (1H, d, J_{gem} = 12 Hz, C$\underline{H}_2$Ph), 4.49 (1H, d, J_{gem} = 12 Hz, C$\underline{H}_2$Ph), 4.59 (1H, d, J_{gem} = 12 Hz, C$\underline{H}_2$Ph), 4.17 (1H, s, H3), 3.75 (1H, d, J_{gem} = 11 Hz, H5), 3.68 (1H, d, J_{gem} = 11 Hz, H5′), 3.38 (3H, s, OC$\underline{H}_3$), 2.2 (1H, s, H2), 1.98 (1H, m, H6), 1.55 (1H, dd, J_{gem} = 12.5 Hz, $J_{6,7}$ = 5 Hz, H6′), 1.88 (1H, m, H7), 1.19 (3H, d, J = 7 Hz, C$\underline{H}_3$); ^{13}C NMR (125 MHz) δ 138.3, 138.6 (aromatic), 128.3, 127.6, 127.4, 127.3 (aromatic), 106.5 (C1), 86.7 (C4), 82.3 (C3), 73.5 (C$\underline{H}_2$Ph), 71.8 (C$\underline{H}_2$Ph), 68.9 (C5), 54.7 (O$\underline{C}H_3$), 48.8 (C2), 38.8 (C6), 32.6 (C7), 20.4 (C$\underline{H}_3$); MALDI-TOF m/z $[M + Na]^+$ calcd for $C_{23}H_{28}NaO_4$ 391.189, found 391.190.

(2*R*,3*S*,4*R*,7*R*)-3-Benzyloxy-5-benzyloxymethyl-4-hydroxy-7-methylcyclopentane-1-carbaldehyde (5). To a solution of **4** (900 mg, 2.4 mmol) in the mixed solvent of THF (30 mL) and H_2O (3 mL) was added *p*-toluenesulfonic acid·H_2O (1.8 g, 9.6 mmol) at room temperature and stirred overnight. The reaction mixture was quenched with saturated solution of $NaHCO_3$, and the aqueous layer was extracted with EtOAc. The combined organic layer was washed with brine, dried over $MgSO_4$, and concentrated under reduced pressure. The residue was filtered by column chromatography (25−30% EtOAc in petroleum ether, v/v) to give **5** as a colorless crude oil (675 mg, 78%), which was used as-is for the next step for Grignard reaction (to compound **6**) because this aldehyde decomposed on standing and also during attempts at mass spectrography: ^{1}H NMR (500 MHz, $CDCl_3$) δ 9.77 (~1H, d, $J_{1,2}$ = 3 Hz, H1), 7.17−7.29 (10H, m, aromatic), 4.41−4.45 (4H, m, 2 × C$\underline{H}_2$Ph), 4.15 (1H, d, $J_{3,2}$ = 4.2 Hz, H3), 3.67 (1H, d, J_{gem} = 9.6 Hz, H5), 3.40 (1H, d, J_{gem} = 9 Hz, H5′), 2.22 (1H, dd, $J_{2,3}$ = 4.8 Hz, H2), 2.49 (1H, m, H7), 2.11 (1H, dd, J_{gem} = 13.8 Hz, $J_{6,7}$ = 9 Hz, H6), 1.09 (1H, dd, J_{gem} = 13.2 Hz, $J_{6,7}$ = 7.2 Hz, H6′), 1.07 (3H, d, J = 5.4 Hz, C$\underline{H}_3$).

(1*S*,2*R*,3*S*,4*R*,7*R*)-3-Benzyloxy-5-benzyloxymethyl-1-hydroxyl-1-*C*-vinyl-7-methylcyclopentane-4-ol (6). Compound **5** (650 mg) was dissolved in THF (20 mL) under nitrogen and cooled to 0 °C. Vinylmagnesium bromide (1.0 M solution in THF, 7.3 mL, 7.3 mmol) was added, and then it was allowed to warm to room temperature and kept stirring at this temperature overnight. The reaction was quenched with water slowly. The residue was diluted with CH_2Cl_2, washed with saturated $NaHCO_3$, dried over $MgSO_4$, and concentrated under reduced pressure. The crude material was purified by column chromatography on silica gel (10−30% ethyl acetate in petroleum ether, v/v) to give **6** as a colorless oil (500 mg, 71%): ^{1}H NMR (600 MHz, $CDCl_3$) δ 7.18−7.28 (10H, m, aromatic), 5.73 (1H, m, H8), 5.23 (1H, dt, J = 1.8 Hz, H9), 5.05 (1H, dt, J = 1.8 Hz, H9′), 4.53 (1H, d, J_{gem} = 16.2 Hz, C$\underline{H}_2$Ph), 4.47 (1H, d, J_{gem} = 16.2 Hz, C$\underline{H}_2$Ph), 4.51 (1H, d, J_{gem} = 12 Hz, C$\underline{H}_2$Ph), 4.44 (1H, d, J_{gem} = 12 Hz, C$\underline{H}_2$Ph), 4.23 (1H, app t, $J_{1,2}$ = 5.4 Hz, $J_{1,8}$ = 6 Hz, H1), 3.95 (1H, d, $J_{3,2}$ = 6 Hz, H3), 3.67 (1H, d, J_{gem} = 9 Hz, H5), 3.37

dx.doi.org/10.1021/jo300936g | J. Org. Chem. 2012, 77, 6855−6872

(1H, d, J_{gem} = 9 Hz, H5′), 2.18 (1H, m, H7), 2.04 (1H, dd, J_{gem} = 11.4 Hz, $J_{6,7}$ = 3 Hz, H6), 1.92 (1H, dd, $J_{2,3}$ = 6 Hz, H2), 1.44 (1H, dd, J_{gem} = 14.4 Hz, $J_{6,7}$ = 6 Hz, H6), 1.04 (3H, d, J = 7.2 Hz, 7-CH_3); ^{13}C NMR (150 MHz) δ 140.6 (C8), 138.3, 138.0, 128.9, 128.8, 128.4, 128.2 (aromatic), 115.2 (C9), 89.1 (C3), 82.4 (C4), 74.5 (CH_2Ph), 74.1 (CH_2Ph), 72.6 (C5), 72.2 (C1), 52.4 (C2), 42.2 (C6), 32.0 (C7), 16.7 (7-CH_3); MALDI-TOF m/z [M + Na]$^+$ calcd for $C_{24}H_{30}NaO_4$ 405.204, found 405.203.

(1*S*,2*R*,3*S*,4*R*,7*R*)-3-Benzyloxy-5-benzyloxymethyl-1-[(4-methoxyphenyl)methoxy]-1-*C*-vinyl-7-methylcyclopentane-4-ol (7). Compound **6** (350 mg, 0.92 mmol) was dissolved in dry DMF (10 mL) cooled to 0 °C. NaH (0.043 g, 1.84 mmol) was added, left to stir for 1 h, PMB-Cl (0.16 mL, 1.2 mmol) was added, and then it was allowed to warm to room temperature and kept stirring at this temperature for 5 h. The reaction was quenched with water slowly. The residue was diluted with EtOAc, washed with brine, dried over $MgSO_4$, and concentrated under reduced pressure. The residue was purified by silica gel column chromatography (10% EtOAc in petroleum ether, v/v) to give **7** as a colorless oil (300 mg, 65%): ^{1}H NMR (500 MHz, $CDCl_3$) δ 7.15−7.22 (13H, m, aromatic), 6.76 (1H, d, J = 8.4 Hz, aromatic), 5.73 (1H, m, $J_{H8,\ H9}$ = 17.5 Hz, $J_{H8,\ H9'}$ = 10.5 Hz, H8), 5.17 (2H, m, $J_{H9,\ H9'}$ = 6.5, H9, H9′), 4.52 (1H, d, J_{gem} = 12 Hz, CH_2Ph), 4.41 (1H, d, J_{gem} = 12 Hz, CH_2Ph), 4.43 (1H, d, J_{gem} = 10.8 Hz, CH_2PMB), 4.16 (1H, d, J_{gem} = 10.8 Hz, CH_2PMB), 4.49 (2H, s, CH_2Ph), 4.04 (1H, d, $J_{3,2}$ = 4 Hz, H3), 3.95 (1H, dd, $J_{1,2}$ = 3.5 Hz, $J_{1,8}$ = 7.5 Hz, H1), 3.72 (3H, s, OCH_3), 3.59 (1H, d, J_{gem} = 9.6 Hz, H5), 3.46 (1H, d, J_{gem} = 9 Hz, H5′), 2.21 (1H, m, $J_{H2,H7}$ = 8.5 Hz, H7), 1.91 (2H, m, H2, H6), 1.37 (1H, dd, J_{gem} = 13.2 Hz, $J_{6,7}$ = 9.6 Hz, H6′), 0.96 (3H, d, $J_{7\text{-}Me,7}$ = 7.2 Hz, 7-CH_3); ^{13}C NMR (150 MHz) δ 159.2 (aromatic), 137.8 (C8), 129.0, 129.7, 128.9, 128.4, 128.3, 128.2, 128.0, 127.7, 127.3 (aromatic), 117.1 (C9), 87.7 (C3), 82.2 (C4), 79.3 (C1), 73.6 (CH_2Ph), 73.0 (C5), 72.3 (CH_2Ph), 70.1 (CH_2PMB), 55.3 (OCH_3), 52.4 (C2), 44.9 (C6), 32.5 (C7), 16.0 (7-CH_3); MALDI-TOF m/z [M + Na]$^+$ calcd for $C_{32}H_{38}NaO_5$ 525.262, found 525.262.

(1*S*,2*R*,3*S*,4*R*,7*R*)-3-Benzyloxy-5-benzyloxymethyl-1-[(4-methoxyphenyl)methoxy]-1-*C*-vinyl-7-methylcyclopentyl methyl oxalate (8). Methyl oxalyl chloride (0.29 mL, 3.18 mmol) was added to a solution of compound 7 (200 mg, 0.39 mmol) in dry pyridine (10 mL) under nitrogen. The mixture was stirred at 40 °C overnight. The reaction was cooled, and the solvent was removed. The residue was extracted with CH_2Cl_2 and saturated $NaHCO_3$ solution. The organic layer was dried over $MgSO_4$ and evaporated. The residue was purified by silica gel column chromatography (0−10% ethyl acetate in petroleum ether, v/v) to obtain **8** as a yellowish oil (160 mg, 68%): ^{1}H NMR (600 MHz, $CDCl_3$) δ 7.13−7.23 (15H, m, aromatic), 6.76 (1H, d, J = 8.4 Hz, aromatic), 5.73 (1H, m, $J_{H1,H8}$ = 7.5 Hz, $J_{H8,H9}$ = 18 Hz, $J_{H8,H9'}$ = 11.5 Hz, H8), 5.17 (2H, m, H9, H9′), 5.17 (1H, d, J_{gem} = 10.8 Hz, CH_2Ph), 4.46 (1H, d, J_{gem} = 10.8 Hz, CH_2Ph), 4.38 (5H, m, CH_2Ph, CH_2PMB, H3), 4.15 (1H, d, J_{gem} = 12 Hz, H5), 4.01 (1H, d, J_{gem} = 12 Hz, H5′), 3.87 (1H, dd, $J_{1,2}$ = 4.8 Hz, $J_{1,8}$ = 7.8 Hz, H1), 3.79 (3H, s, OCH_3), 3.73 (3H, s, OCH_3), 2.27 (1H, dd, J_{gem} = 13.2 Hz, $J_{6,7}$ = 7.2 Hz, H6), 2.15 (1H, m, H7), 2.06 (1H, m, H2), 1.95 (1H, dd, J_{gem} = 13.8 Hz, $J_{6,7}$ = 8.4 Hz, H6′), 0.94 (3H, d, J = 6.6 Hz, CH_3); ^{13}C NMR (150 MHz) δ 159.3, 159.3 (C═O), 156.8 (aromatic), 138.4 (C8), 131.1, 128.7, 128.5, 128.0, 127.8, 127.7, 114.0 (aromatic), 117.7 (C9), 94.9 (C4), 86.6 (CH_2Ph), 79.9 (C1), 73.8 (CH_2Ph), 72.5 (CH_2PMB), 69.7 (C5), 55.7, 53.7 (OCH_3), 52.2 (C2), 42.2 (C6), 30.1 (C7), 16.6 (CH_3); MALDI-TOF m/z [M + Na]$^+$ calcd for $C_{35}H_{40}NaO_8$ 611.262, found 611.265.

(1*S*,2*R*,3*S*,4*R*,7*R*,8*R*)-3-(Benzyloxy)-4-(benzyloxymethyl)-1-[(4-ethyloxyphenyl)methoxy]-8,7-dimethylbicyclo[2.2.1]-heptane (9). Compound **8** (100 mg, 0.17 mmol) was dissolved in 6 mL of anhydrous toluene to which N_2 was purged for 30 min. The mixture was heated to reflux, and Bn_3SnH (0.19 mL in 2 mL of anhydrous toluene) and AIBN (30 mg in 2 mL of anhydrous toluene) were added dropwise in 2 h and reflux was continued for 2 h. Solvent was evaporated, and the concentrate was purified by silica gel column chromatography (0−5% EtOAc in petroleum ether, v/v) to give compound **9** as a colorless oil (50 mg, 60%): ^{1}H NMR (600 MHz, $CDCl_3$) δ 7.18−7.26 (15H, m, aromatic), 6.79 (2H, d, 8.4, aromatic), 4.44 (1H, d, J_{gem} = 11 Hz, CH_2PMB), 4.43 (2H, s, CH_2Ph), 4.38 (1H, d, J_{gem} = 12 Hz, CH_2Ph), 4.27 (1H, d, J_{gem} = 12 Hz, CH_2Ph), 4.23 (1H, d, J_{gem} = 11.4 Hz, CH_2PMB), 3.72 (3H, s, OCH_3), 3.50 (1H, d, J_{gem} = 9 Hz, H5), 3.41 (1H, d, J_{gem} = 8.4 Hz, H5′), 3.41 (1H, s, H3), 3.32 (1H, t, $J_{1,8}$ = 5, $J_{1,2}$ = 3.5 Hz, H1), 2.46 (1H, m, $J_{2,7}$ = 5.4 Hz, H7), 2.43 (1H, d, $J_{2,3}$ = 4 Hz, H2), 2.08 (1H, t, $J_{6,6'}$ = 11.4 Hz, $J_{6,7}$ = 11, Hz, H6), 1.65 (1H, t, H8), 1.25 (3H, d, J = 5.4 Hz, 7-CH_3), 1.14 (1H, dd, J_{gem} = 12 Hz, $J_{6,7}$ = 5.4 Hz, H6′), 0.92 (3H, d, J = 7.2 Hz, 8-CH_3); ^{13}C NMR (150 MHz) δ 159.0, 138.8, 130.9, 128.9, 128.2, 127.4, 127.3, 127.1, 113.7 (aromatic), 87.0 (C1), 84.2 (C3), 73.4 (CH_2Ph), 71.1 (C5), 70.8 (CH_2Ph), 55.3 (OCH_3), 53.0 (C4), 45.3 (C2), 45.0 (C8), 42.0 (C6), 31.4 (C7), 17.6, 17.5 (CH_3); MALDI-TOF m/z [M + Na]$^+$ calcd for $C_{32}H_{38}NaO_4$ 509.267, found 509.268.

3,5-Di-*O*-benzyl-6-*O*-mesyl-1-*O*-methyl-β-D-ribofuranose 12. Compound **10** (500 mg, 1.25 mmol) was dissolved in dry pyridine (8 mL). Methanosulfonyl chloride (145 μL, 1.87 mmol) was added at 0 °C. The reaction was stirred at room temperature for 1 h. The reaction mixture was partitioned between EtOAc and H_2O. The organic layer was washed with brine twice and dried over anhydrous sodium sulfate, filtered, and concentrated in vacuo to give crude **11** (as a yellowish oil) which then was dissolved in MeOH (8 mL), and *p*-toluenesulfonic acid·H_2O (500 mg) was added at room temperature. The reaction mixture was stirred at rt overnight. The mixture was diluted with dichloromethane and washed with $NaHCO_3$, dried over anhydrous sodium sulfate, filtered, and evaporated. The crude **12** was purified by silica gel column chromatography (10−40% EtOAc/petroleum ether) to yield **12** as a colorless oil (520 mg, 92%): ^{1}H NMR (600 MHz, $CDCl_3$) δ 7.31−7.23 (10H, m, aromatic H), 4.86 (1H, s, H1), 4.64 (1H, d, J = 11.4 Hz, H5), 4.59 (2H, d, J = 11.4 Hz, CH_2Ph), 4.55 (1H, d, J_{gem} = 11.4 Hz, H5′), 4.51 (1H, d, J_{gem} = 10.8 Hz, CH_2Ph), 4.42 (1H, d, J = 10.8 Hz, CH_2Ph), 4.22 (1H, d, $J_{3,2}$ = 4.8 Hz, H3), 4.04 (1H, t, H2), 3.69 (1H, d, J = 9 Hz, H6), 3.34 (1H, d, H6′), 3.28 (3H, s, OMe), 2.98 (3H, s, Mesyl-CH_3), 2.72 (1H, d, OH); ^{13}C NMR (150 MHz, $CDCl_3$) δ 137.6, 137.3, 128.7, 128.6, 128.5, 128.3, 128.1, 128.0, 127.9, 127.8 (aromatic C), 107.5 (C1), 83.2 (C4), 81.9 (C3), 74.1 (C5), 73.7 (C2), 73.4 (C6), 72.5 (CH_2Ph), 70.6 (CH_2Ph), 54.9 (CH_3), 37.2 (CH_3); MALDI-TOF m/z [M + Na]$^+$ calcd for $C_{22}H_{28}NaO_8S$ 475.140, found 475.140.

(1*R*,2*R*,3*R*,4*R*)-3-Benzyloxy-4-benzyloxymethyl-1-methoxy-2-oxabicyclo[2.2.1.]heptane 13. Compound **12** (520 mg, 1.15 mmol) was dissolved in MeOH (20 mL). Potassium carbonate (190 mg, 1.39 mmol) was added at 0 °C. The reaction was left to stir at 5 °C overnight. The temperature was raised to room temperature, at which the reaction mixture was stirred for another hour. MeOH was evaporated, and the mixture was dissolved in EtOAc and washed with H_2O. The aqueous layer was extracted with EtOAc again, dried over anhydrous sodium sulfate, filtered, and evaporated in vacuo. The crude compound **13** was purified by silica gel column chromatography (5−15% EtOAc/petroleum ether) to give **13** as a colorless oil (305 mg, 74%): ^{1}H NMR (500 MHz, $CDCl_3$) δ 7.34−7.26 (10H, m, aromatic H), 4.81 (1H, s, H1), 4.65(1H, d, J_{gem} = 12 Hz, CH_2Ph), 4.61 (2H, s, CH_2Ph), 4.56 (1H, d, J_{gem} = 12 Hz, CH_2Ph), 4.11 (1H, s, H3), 4.08 (1H, s, H2), 4.00 (1H, d, J = 7.5 Hz, H5), 3.81−3.75 (3H, m, H6, H6′, H5′), 3.39 (3H, s, CH_3); ^{13}C NMR (125 MHz, $CDCl_3$) δ 137.9, 128.4, 127.8, 127.7, 127.6 (aromatic C), 104.9 (C1), 85.2 (C4), 79.2 (C2), 76.8 (C3), 73.7 (CH_2Ph), 72.3 (C5), 72.2 (CH_2Ph), 66.6 (C6), 55.4 (CH_3); MALDI-TOF m/z [M + Na]$^+$ calcd for $C_{21}H_{24}NaO_5$ 379.152, found 379.152.

(2*R*,3*R*,4*R*)-3-(Benzyloxy)-4-[(benzyloxy)methyl]-tetrahydro-4-hydroxyfuran-2-carbaldehyde 14. To compound **13** (300 mg, 0.84 mmol) in THF (10 mL) were added *p*-toluenesulfonic acid·H_2O (641 mg, 3.37 mmol) and distilled H_2O (1 mL). The reaction was stirred at room temperature overnight. The mixture was then quenched with saturated $NaHCO_3$ solution, extracted with EtOAc, dried over anhydrous sodium sulfate, filtered, and evaporated. The crude aldehyde was purified by silica gel column chromatography (20−40% EtOAc/petroleum ether) to give **14** as a yellowish oil (252 mg, 75%): ^{1}H NMR (500 MHz, $CDCl_3$) δ 9.56 (1H, s, aldehyde), 7.28−7.18 (10H, m, H aromatic), 4.61 (1H, d, CH_2Ph), 4.51 (2H, m, CH_2Ph), 5.38 (1H, m, CH_2Ph), 4.32 (1H, s, H2), 3.91 (3H, m, H3, H6), 3.78 (1H, d, J_{gem} = 9.5 Hz, H5), 3.44 (1H, d, H5′); MALDI-TOF m/z [M + Na]$^+$ calcd for $C_{20}H_{22}NaO_5$ 365.136, found 365.137.

(1*R*,2*R*,3*R*,4*R*)-3-(Benzyloxy)-4-[(benzyloxy)methyl]-tetrahydro-5-(1-hydroxyallyl)-furan-3-ol 15. To the aldehyde **14** (210 mg,

dx.doi.org/10.1021/jo300936g | J. Org. Chem. 2012, 77, 6855−6872

0.61 mmol) in dry THF (3 mL) was added vinylmagnesium bromide (1 M in THF, 2.5 mL, 2.5 mmol) at 0 °C. The reaction was stirred at room temperature overnight. The reaction mixture was the quenched with saturated $NaHCO_3$ solution, extracted with EtOAc, dried over anhydrous sodium sulfate, filtered, and evaporated. The crude **15** was purified by silica gel column chromatography (20−50% EtOAc/petroleum ether) to yield **15** as a yellowish oil (140 mg, 62%): ^{1}H NMR (500 MHz, $CDCl_3$) δ 7.38−7.28 (10H, m, aromatic H), 5.92 (1H, m, $J_{7,8}$ = 10.5 Hz, H7), 5.38 (1H, dd, $J_{8,8'}$ = 17 Hz, H8), 5.24 (1H, dd, $J_{8,8'}$ = 10.5 Hz, H8′), 4.64 (2H, s, CH_2Ph), 4.59 (2H, m, CH_2Ph), 4.19 (1H, dt, $J_{1,2}$ = 5 Hz, $J_{1,7}$ = 5.5 Hz, H1), 3.94 (1H, m, $J_{2,3}$ = 3 Hz, H2), 3.90 (1H, m, H3), 3.89−3.82 (3H, m, H6, H5), 3.63 (1H, d, J_{gem} = 9.5 Hz, H6′); ^{13}C NMR (125 MHz, $CDCl_3$) δ 138.1 (C7), 129.0, 128.9, 128.4, 128.3 (C aromatic), 117.3 (C8), 88.0 (C2), 85.6 (C3), 82.0 (C4), 75.5 (C5), 74.3 (CH_2−Ph), 73.6 (C1), 72.9 (CH_2−Ph), 70.0 (C6); MALDI-TOF m/z $[M + Na]^+$ calcd for $C_{22}H_{26}NaO_5$ 393.168, found 393.168.

(1*R*,2*R*,3*R*,4*R*)-5-(1-(4-Methoxybenzyloxy)allyl)-3-(benzyloxy)-4-[(benzyloxy) methyl]tetrahydrofuran-3-ol 16. Compound **15** (80 mg, 0.22 mmol) was dissolved in dry DMF (3 mL). Then, 60% NaH (17 mg, 0.432 mmol) was added at 0 °C and left to stir at room temperature for 30 min at which PMB-Cl (38 μL, 0.28 mmol) was added at 0 °C. The reaction was left to stir at room temperature for 3 h. Brine was added to the reaction mixture, extracted with EtOAc, dried over anhydrous sodium sulfate, filtered, and evaporated followed by purification by silica gel column chromatography (5−15% EtOAc/petroleum ether) to yield **16** as a yellowish oil (75 mg, 71%): ^{1}H NMR (500 MHz, $CDCl_3$) δ 7.27−7.09 (12H, m, aromatic H), 6.79 (2H, d, J = 8.4 Hz, H- PMB), 5.84 (1H, m, $J_{7,8}$ = 10.5 Hz, H7), 5.30 (1H, d, $J_{7,8}$ = 10.0 Hz, H8), 5.22 (1H, dd, $J_{8',8}$ = 1 Hz, H8′), 4.54 (2H, s, CH_2Ph), 4.52 (1H, d, J_{gem} = 11.4 Hz, CH_2PMB), 4.45 (1H, d, J_{gem} = 12 Hz, CH_2Ph), 4.34 (1H, d, J_{gem} = 12 Hz, CH_2Ph), 4.21 (1H, d, J_{gem} = 11.4 Hz, CH_2PMB), 3.80 (1H, t, $J_{2,3}$ = 3 Hz, H2), 3.77 (1H, d, J_{gem} = 9.6 Hz, H5), 3.72 (3H, s, CH_3PMB), 3.72−3.69 (4H, m, H3, H6, H5′), 3.64 (1H, dd, $J_{1,2}$= 3.5 Hz, $J_{1,7}$= 7.8 Hz, H1), 3.59 (1H, d, J_{gem} = 9.6 Hz, H6′); ^{13}C NMR (125 MHz, $CDCl_3$) δ 135.2 (C7), 129.9, 129.5, 128.4, 127.9, 127.7 (C aromatic), 119.4 (C8), 113.8 (CH_2−PMB), 87.4 (C2), 85.7 (C3), 81.4 (C4), 79.3 (C1), 75.6 (C5), 73.9 (CH_2−Ph), 72.7 (CH_2−Ph), 69.9 (C6), 55.3 (C-Me); MALDI-TOF m/z $[M + Na]^+$ calcd for $C_{30}H_{34}NaO_6$ 513.225, found 513.226.

(1*R*,2*R*,3*R*,4*R*)-5-(1-(4-Methoxybenzyloxy)allyl)-3-(benzyloxy)-4((benzyloxy)methyl)tetrahydrofuran-3-yl methyl oxalate 17. Methoxyoxalyl chloride (38 μL, 0.41 mmol) was added to a solution of **16** (50 mg, 0.1 mmol) in dry pyridine (3 mL). The reaction was stirred at 50 °C overnight at which time it was quenched with saturated $NaHCO_3$ solution, extracted with DCM, dried over anhydrous sodium sulfate, filtered, and evaporated. The crude **17** was purified by silica gel column chromatography (5−15% EtOAc/petroleum ether) to yield **17** as a colorless oil (40 mg, 73%): ^{1}H NMR (500 MHz, $CDCl_3$) δ 7.21−7.11 (12H, aromatic H), 6.78 (2H, d, J = 9 Hz, CH_2-PMB), 5.78 (1H, m, H7), 5.25 (1H, d, J = 7 Hz, H8), 5.21 (1H, s, H8′), 4.59 (1H, d, J_{gem} = 11.5 Hz, CH_2Ph), 4.49 (1H, d, J_{gem} = 11.5 Hz, CH_2PMB), 4.47 (2H, ABq, J_{gem} = 12 Hz, CH_2Ph), 4.35 (1H, d, J_{gem} = 11.0 Hz, H6), 4.29 (1H, d, J_{gem} = 11.5 Hz, CH_2Ph), 4.15 (3H, m, H2, H5, H6), 3.89 (1H, d, J_{gem} = 10.5 Hz, H5′), 3.80 (4H, m, CH_3, H6′), 3.75 (2H, m, H3, H1), 3.70 (3H, s, CH_3PMB); ^{13}C NMR (125 MHz, $CDCl_3$) δ 159.2, 157.9, (C═O), 137.7 (C7), 134.9, 129.7, 128.4, 128.0, 127.8, 127.7 (C aromatic), 119.3 (C8), 113.7 (C-PMB), 92.8 (C4), 86.5 (C3), 83.4 (C2), 78.4 (C1), 73.9 (CH_2−Ph), 73.6 (C6), 73.3 (CH_2−Ph), 70.0 (CH_2−PMB), 66.4 (C5), 55.3 (OCH_3−PMB), 53.5 (CH_3); MALDI-TOF m/z $[M + Na]^+$ calcd for $C_{33}H_{36}NaO_9$ 599.136, found 599.134.

(1*R*,2*R*,3*R*,4*R*,7*S*)-3-(Benzyloxy)-4-[(benzyloxy)methyl]-1-[(4-methoxyphenyl)methoxy]-7-methyl-2-oxabicyclo[2.2.1]-heptane18a and (1*R*,2*R*,3*R*,4*R*,7*R*)-3-(Benzyloxy)-4-[(benzyloxy)methyl]-1-[(4methoxyphenyl)methoxy]-7-methyl-2-oxabicyclo[2.2.1]heptane 18b. Compound **17** (20 mg, 0.036 mmol) was dissolved in dry toluene (2 mL). Bu_3SnH (40 μL, 0.146 mmol in 0.5 mL of dry toluene) and AIBN (5.9 mg, 0.036 mmol in 0.5 mL of dry toluene) were added over 1 h at reflux. The reaction was stirred at reflux for another 2 h at which time the mixture was evaporated in vacuo. The crude **18a**/**18b** was purified by silica gel column chromatography (5−20% EtOAc/petroleum ether) to yield **18a**/**18b** as a yellowish oil (8 mg, 47%). Major isomer: ^{1}H NMR (500 MHz, $CDCl_3$) δ 7.26−7.12 (12H, m, aromatic H), 6.80 (2H, d, CH_2-PMB, J = 8.5 Hz), 4.57 (1H, d, J_{gem} = 12 Hz, CH_2Ph), 4.50 (1H, d, J_{gem} = 12 Hz, CH_2Ph), 4.47 (1H, d, J_{gem} = 12.5 Hz, CH_2Ph), 4.42 (1H, d, J_{gem} = 11.5 Hz, CH_2Ph), 4.39 (2H, m, CH_2PMB), 3.95 (1H, br s, H2), 3.89 (1H, s, H3), 3.74 (3H, s, CH_3), 3.58 (3H, m, H5, H5′, H6), 3.36 (1H, d, J = 9.5 Hz, H6′), 3.09 (1H, dd, $J_{1,7}$ = 3 Hz, H1), 2.03 (1H, m, $J_{7,1}$ = 3 Hz, H7), 0.98 (3H, d, $J_{8,7}$ = 7 Hz, H8); ^{13}C NMR (125 MHz, $CDCl_3$) δ 159.2 (C-PMB), 138.5, 138.4, 138.3, 130.7, 129.5, 129.2, 128.3, 127.7, 127.5 (C aromatic), 113.8 (C-PMB), 84.3 (C1), 82.3 (C3), 78.4 (C2), 73.3 (CH_2Ph), 71.9 (CH_2Ph), 71.1 (CH_2PMB), 66.3 (C6), 65.3 (C5), 55.3 (CH_3), 52.4 (C4), 39.8 (C7), 12.9 (C8); MALDI-TOF m/z $[M + Na]^+$ calcd for $C_{30}H_{34}NaO_5$ 497.233, found 497.231. Minor isomer: ^{1}H NMR (500 MHz, $CDCl_3$) δ 7.20−7.21 (m, aromatic H), 4.51−4.41 (6H, m, 2 × CH_2Bn, CH_2PMB), 3.93 (1H, s, H2), 3.71 (1H, s, H3), 3.092 (1H, m, $J_{1,7}$ = 8 Hz, H1), 2.03 (1H, m, H7), 0.91 (3H, d, J = 7.5 Hz, H8); ^{13}C NMR (125 MHz, $CDCl_3$) δ 159.1 (C-PMB), 138.4, 138.3, 130.7, 129.5, 129.2, 128.9, 128.3, 127.6, 127.5 (C aromatic), 84.3 (C1), 82.3 (C3), 78.4 (C2), 73.3 (CH_2Ph), 71.9 (CH_2Ph), 71.1 (CH_2PMB), 66.3 (C6), 65.3 (C5), 55.3 (CH_3), 52.4 (C4), 39.8 (C7), 12.9 (C8); MALDI-TOF m/z $[M + Na]^+$ calcd for $C_{30}H_{34}NaO_5$ 497.233, found 497.231.

■ ASSOCIATED CONTENT

Supporting Information

^{1}H, ^{13}C NMR, COSY, HMQC, HMBC spectra for compounds **1**−**9** (Supporting Information part I) and **10**−**18a**/**18b** (part II); ^{1}H homodecoupling for compounds **7**, **8**, and **9** (part I), **15**, **16**, and **18a**/**18b** (part II); 1D NOE spectra for compounds **7**, **8**, and **9** (part I), **12**, **15**, **16**, and **18a**/**18b** (part II) and $^3J_{HH}$ vicinal coupling constant of compounds **7**, **8**, and **9** (part I), **15**, **16**, and **18a**/**18b** (part II) along with Newman projections of these compounds; molecular structures based on MM and semi-empirical calculations for compounds **7**, **8**, and **9** (part I), **12**, **16**, and **18a**/**18b** (part II). This material is available free of charge via the Internet at http://pubs.acs.org.

■ AUTHOR INFORMATION

Corresponding Author

*E-mail: jyoti@boc.uu.se.

Notes

The authors declare no competing financial interest.

■ ACKNOWLEDGMENTS

M.K. and S.E. have contributed equally. Generous financial support is from the Swedish Natural Science Research Council (Vetenskapsrådet), the Swedish Foundation for Strategic Research (Stiftelsen för Strategisk Forskning), and the EU-FP6 funded RIGHT project (Project No. LSHB-CT-2004-005276). M.K. and S.E. also thank Dr. O. Plashkevych of this lab for teaching them to use the HyperChem program.

■ REFERENCES

(1) (a) Obika, S.; Nanbu, D.; Hari, Y.; Morio, K.; In, Y.; Ishida, T.; Imanishi, T. *Tetrahedron Lett.* **1997**, *38*, 8735−8738. (b) Singh, S. K.; Nielsen, P.; Koshkin, A. A.; Wengel, J. *Chem. Commun.* **1998**, *4*, 455−456. (c) Chuanzheng, Z.; Chattopadhyaya, J. *Chem. Rev.* **2012**, *112*, 3808−3832. (d) Srivastava, P.; Barman, J.; Pathmasiri, W.; Plashkevych, O.; Wenska, M.; Chattopadhyaya, J. *J. Am. Chem. Soc.* **2007**, *129*, 8362−8379. (e) Zhou, C.; Liu, Y.; Andaloussi, M.; Badgujar, N.; Plashkevych, O.; Chattopadhyaya, J. *J. Org. Chem.* **2009**, *74*, 118−134. (f) Xu, J.; Liu, Y.; Dupouy, C.; Chattopadhyaya, J. *J. Org. Chem.* **2009**, *74*, 6534−6554. (g) Liu, Y.; Xu, J. F.; Karimiahmadabadi, M.; Zhou, C.; Chattopadhyaya, J. *J. Org. Chem.* **2010**, *75*, 7112−7128. (h) Seth, P. P.; Allerson, C. R.; Berdeja, A.; Siwkowski, A.; Pallan, P. S.; Gaus, H.; Prakash, T. P.; Watt,

A. T.; Egli, M.; Swayze, E. E. *J. Am. Chem. Soc.* **2010**, *132*, 14942−14950.
(i) Upadhayaya, R.; Deshpande, S.; Li, Q.; Kardile, R.; Sayyed, A.; Kshirsagar, E.; Salunke, R.; Dixit, S.; Zhou, C.; Földesi, A.; Chattopadhyaya, J. *J. Org. Chem.* **2011**, *76*, 4408−4431.
(2) Dutta, S.; Bhaduri, N; Rastogi, N.; G., Chandel, S.; Vandavasi, J. K.; Upadhayaya, R. S.; Chattopadhyaya, J. *Med. Chem. Commun.* **2011**, *2*, 206−216.
(3) Dutta, S.; Bhaduri, N.; Upadhayaya, R. S.; Rastogi, N.; Chandel, S. G.; Vandavasi, J. K.; Plashkevych, O.; Kardile, R. A.; Chattopadhyaya, J. *Med. Chem. Commun.* **2011**, *2*, 1110−1119.
(4) Gagnon, K. T.; Pendergraff, H. M.; Deleavey, G. F.; Swayze, E. E.; Potier, P.; Randolph, J.; Roesch, E. B.; Chattopadhyaya, J.; Damha, M. J.; Bennett, C. F.; Montaillier, C.; Lemaitre, M.; Corey, D. R. *Biochemistry* **2010**, *49*, 10166−10178.
(5) (a) Marquez, V. E.; Lim, M. *Med. Res. Rev.* **1986**, *6*, 1. (b) Kim, H. S.; Ravi, V.; Marquez, E.; Maddileti, S.; Wihlborg, A. K.; Erlinge, M.; Malmsjo, T. K.; Harden, Boyer, J. L.; Jacobson, K. A. *J. Med. Chem.* **2002**, *45*, 208−218. (c) Shin, K. J.; Moon, H. R.; George, C.; Marquez, V. E. *J. Org. Chem.* **2000**, *65*, 2172−2178. (d) Marquez, V. E.; Lim, M.; Tseng, C. K. H.; Markovac, A.; Priest, M. A.; Sami Khan, M.; Kaskar, B. *J. Org. Chem.* **1988**, *53*, 5709−5714. (e) Marquez, V. E.; Siddiqui, M.; Ezzitouni, A.; Russ, P.; Wang, J.; Wagner, R. W.; Matteucci, M. D. *J. Med. Chem.* **1996**, *39*, 3739−3747. (f) Marquez, V. E.; Lim, M.; Treanor, S. P.; Polwman, J.; Priest, M. A.; Markovac, A.; Sami Khan, M.; Kaskar, B.; Driscoll, J. S. *J. Med. Chem.* **1988**, *31*, 1687−1694.
(6) Jacobson, K. A.; Ji, X. D.; Li, A. H.; Melman, N.; Siddiqi, M. A.; Shin, K. J.; Marquez, V. E.; Ravi, R. G. *J. Med. Chem.* **2000**, *43*, 2196−2203.
(7) (a) Kim, H. S.; Jacobson, K. A. *Org. Lett.* **2003**, *5*, 1665−1668. (b) Jeong, L. S.; Lee, J. A. *Antiviral Chem. Chemother.* **2004**, *15*, 235−250.
(8) Callam, C. S.; Lowary, T. *Org. Lett.* **2000**, *2*, 167−169.
(9) Winkler, J. D.; Sridar, V. *J. Am. Chem. Soc.* **1986**, *108*, 1708−1709.
(10) (a) Contelles, J. M.; Ruiz, P.; Sanchez, B.; Jimeno, M. L. *Tetrahedron Lett.* **1992**, *33*, 5261−5264. (b) Contelles, J. M.; Ruiz, P.; Martinez, L. A.; Grau, M. *Tetrahedron* **1993**, *49*, 6669−6694.
(11) Gomez, A. M.; Company, M. D.; Uriel, C.; Valverde, S.; López, J. *Tetrahedron Lett.* **2007**, *48*, 1645−1649.
(12) Beckwith, A. L. J.; Schiesser, C. H. *Tetrahedron* **1985**, *41*, 3925−3941.
(13) Spellmeyer, D. C.; Houk, K. N. *J. Org. Chem.* **1987**, *52*, 959−974.
(14) (a) Rajan Babu, T. V.; Fukunaga, T.; Reddy, G. S. *J. Am. Chem. Soc.* **1989**, *111*, 1759−1769. (b) Rajan Babu, T. V. *Acc. Chem. Res.* **1991**, *24*, 139−145. (c) Rajan Babu, T. V. *J. Am. Chem. Soc.* **1987**, *109*, 609−611.
(15) Tsuboi, K.; Nakamura, T.; Suzuki, T.; Nakazaki, A.; Kobayashi, S. *Tetrahedron Lett.* **2010**, *51*, 1876−1879.
(16) (a) Chen, Y.; Wang, L.; Li, Y. *Chem.—Eur. J.* **2011**, *17*, 12582−12586. (b) Coates, G. E.; Heslop, J. A. *J. Chem. Soc.* **1968**, *A*, 514−518. (c) http://www.adichemistry.com/organic/organicreagents/grignard/grignard-reagent-reaction-1.html.
(17) Johansson, R. *Carbohydr. Res.* **2012**, *353*, 92−95.
(18) Serebryany, V.; Beigelman, L. *Tetrahedron Lett.* **2002**, *43*, 1983−1985.
(19) Dang, H. S.; Roberts, B. P.; Tocher, D. A. *J. Chem. Soc., Perkin Trans. 1* **2001**, 2452−2461.
(20) *HyperChem Pro 6.0*; Hypercube Inc., Gainesville, FL, 2000.
(21) (a) Navarro-Vazquez, A.; Cobas, J. C.; Sardina, F. J.; Casanueva, J.; Diez, E. *J. Chem. Inf. Comput. Sci.* **2004**, *44*, 1680−1685. (b) Chimiche, R. R.; Ricerche, M. *J. Chem. Inf. Comput. Sci.* **1996**, *36*, 885−887.